N 70 13850

NASA CR 107316

Final Report

for

Ion Microthruster System Investigation
(15 October 1968 to 15 May 1969)

Contract No.: NAS5-11646

CASE FILE COPY

Prepared by
Electro-Optical Systems

for
Goddard Space Flight Center
Greenbelt, Maryland

Final Report
for
Ion Microthruster System Investigation
(15 October 1968 to 15 May 1969)

Contract No.: NAS5-11646

Goddard Space Flight Center

Contracting Officer: Mr. Kent Cockerham, Code 245
Technical Monitor: Dr. R. E. Hunter, Code 734

Prepared by
Electro-Optical Systems
Pasadena, California

Program Manager: R. Worlock

for
Goddard Space Flight Center
Greenbelt, Maryland

ABSTRACT

This report covers a series of investigations into problems encountered in developing and testing contact ion microthruster systems for flight on Applications Technology Satellites D and E. Investigations were made of thruster performance degradation due to contamination of the ionizing surface, selected circuit modifications were made and tested in the control logic and power conditioning unit of the contact ion microthruster systems, and the transient response of the beam control feedback loop was investigated. Results of the investigations have been useful. Although no definite cause can be identified, ionizer contamination appears to be related to contamination of vacuum chamber surfaces exposed to the thruster. Contamination by the control logic and power conditioning package appears unlikely. Circuit modifications that were made and tested have resulted in an improved system. Investigation of feedback loop transient response has improved the understanding of system behavior and identified several areas for attention in future system design. Recommendations include the incorporation of circuit improvement in future systems and consideration of several factors which could contribute to improved feedback loop transient response.

CONTENTS

1. INTRODUCTION 1

2. IONIZER CONTAMINATION INVESTIGATIONS 3

2.1 Historical Background 3

2.2 Technical Background 5

2.3 Program Approach 8

2.4 Experimental Results 10

2.5 Summary of Results 19

3. IONIZER PROTECTIVE COATINGS 20

3.1 Coating Benefits 20

3.2 Coating Requirements and Selection of Coatings 20

3.3 Application of Coatings to Ionizers 23

3.4 Sealing and Evaporation Tests 23

3.5 Performance Tests 26

3.6 1000-Hour Evaluation Test 31

3.7 Summary 33

4. CLPC DESIGN MODIFICATION 37

4.1 Flip-Flop Transient Immunity 37

4.2 Thrust Level Select D-to-A Converter Circuit 41

4.3 Overload and Converter Drive Circuit 42

4.4 Construction and Testing of Breadboarded Modules 46

4.5 Welded Module Fabrication and Final Testing 51

5. BEAM CONTROL LOOP TRANSIENT RESPONSE 54

5.1 Introduction 54

5.2 Control Circuitry Response 54

5.3 Feed System Response 58

6. NEW TECHNOLOGY 68

REFERENCES

FIGURES

1.	Thruster Subsystem SN 15 Critical Temperature	12
2.	Thruster Subsystem SN 15 Perveance	13
3.	Cadmium Deposition Apparatus	27
4.	Critical Temperature Measurement	29
5.	Turn-On Steering Circuit	39
6.	Digital-To-Analog Converter Circuit	43
7.	Overload and Converter Drive Circuit	45
8.	Breadboard A-13	48
9.	Vaporizer Control Circuit Gain and Phase versus Frequency	56
10.	Vaporizer Magamp Transfer Characteristic	57
11.	Vaporizer Gain and Phase versus Frequency	59
12.	Vaporizer Phase Response	61
13.	Vaporizer Amplitude Response	62
14.	Vaporizer Phase Response	63
15.	Vaporizer Amplitude Response	64
16.	Vaporizer Control Loop Gain and Phase Shift Limits	67

TABLES

I	Potential Ionizer Contamination Sources	6
II	Summary: RGA Determinations	17
III	Ionizer Coatings to Be Tested	22
IV	Gas Permeability of Tungsten Buttons	25
V	Critical Temperature Changes	30
VI	1000-Hour Test Results	34
VII	Test Results	36
VIII	Levels Required to Trigger Flip-Flops for Positive Rectangular Pulses on Command Line	38
IX	Output Voltage versus Temperature for D-to-A Converter	42

SECTION 1

INTRODUCTION

In the development, construction, and testing of ion microthruster systems for ATS D and E satellites, a number of problems arose. Because of the press of time, these problems could be dealt with only in a very limited way. Extended investigations into the source of a problem or solutions involving significant changes in system design were not feasible because the program was strictly geared to flight hardware fabrication and acceptance testing on a rapid schedule.

In most cases, an acceptable if not completely satisfactory solution to a problem was arrived at in the limited time available, allowing the program to proceed. When hardware testing and delivery were completed, it was felt that it would be highly desirable to conduct further investigations of selected problems, determining the cause of the problem whenever possible, and presenting the available solutions. These investigations would increase understanding of the ATS D and E units and provide information useful in development of future systems.

This report covers the work accomplished on the resulting program which was titled, "Ion Microthruster System Investigations." The program was divided into three areas of investigation. The first of these areas, ionizer contamination, was investigated because of microthruster system malfunctions which suggested that the ionizing surface had become contaminated. The goal was to identify the source of contamination and suggest procedures for avoiding it. An additional part of this investigation was the evaluation of coatings which might be used to protect ionizers from contamination during nonoperating periods.

The second area involved the design and testing of selected circuit design changes in the control logic and power conditioning unit. The purpose of these changes is to reduce the noise susceptibility of counter circuits which determine thrust level and thrust deflection, insure initial turn-on of these counters to a predetermined state, and increase the repeatability and stability of the high voltage overload circuits.

The third area was an investigation of the transient response of the beam control loop, prompted by occasional instances of loop instability. By measuring, separately, the responses of the beam control circuitry and the feed system, necessary information for obtaining improved loop response and stability may be obtained.

This report describes the rationale, the approach taken, and the results obtained for each area of investigation.

SECTION 2

IONIZER CONTAMINATION INVESTIGATIONS

2.1 HISTORICAL BACKGROUND

During thruster system development and in qualification testing for the ATS microthruster program, several thrusters exhibited characteristics which are consistent with those expected if the porous tungsten ionizing surface becomes contaminated. This problem area was unanticipated since it had not been encountered in years of laboratory operation of contact ion thrusters and in the operation of fully integrated flight test systems. More recently, operation of a 10 micropound system and development of the thruster subsystem for the ATS system had proceeded smoothly.

The problem first arose when the thruster was assembled with the prototype control logic and power conditioning (CLPC) unit for system tests. It was found that the system operated normally at ion beam currents up to and including approximately 0.75 mA. (For a source 0.187 inches in diameter, this corresponds to a current density of 4.2 mA/cm^2.) When the cesium vapor feed rate was increased in an attempt to increase the beam current to 1 mA (5.6 mA/cm^2), the current handling capability of the ionizer at its operating temperature of approximately 1060°C was apparently exceeded. Instead of continuing to increase, the ion beam current reached a peak, then decreased markedly. The decrease in ion beam current was accomplished by an increase in accelerator drain current, lending support to the explanation that the drop in beam current was associated with a change in the operating characteristics of the ionizer.

This behavior was observed consistently with several ionizers, each of which had previously operated in a satisfactory way using laboratory power supplies. The conclusion drawn at that time was that the ionizer surface was being contaminated and the power conditioning unit was the source of the contamination. Since it was required that the entire package be vented to space through the thruster nozzle, pumpout tubes from the high voltage and low voltage compartments of the power conditioning unit were carried through the thruster compartment and exhausted near the end of the thruster housing. Although the vast majority of any gases evolved by the power conditioning unit could be expected to travel immediately to the test chamber and ultimately to its pumping system, there existed the possibility that a small fraction might impinge on the ionizer surface. A series of tests was conducted in which the power conditioning unit and thruster were isolated. The results indicated that if the two portions of the system could be adequately isolated, the contamination problem would be solved. On this basis, ATS Project Management authorized venting of the power conditioning unit into the interior of the spacecraft. The microthruster system design was changed accordingly; the vent tubes into the thruster compartment were sealed and vent holes were drilled into the housing of the power conditioning unit.

This design was used in the fabrication of both qualification and flight model microthruster systems. When qualification testing was begun, it was discovered that the problem had not been solved. Although full thrust of 20 micropounds could occasionally be produced, the system commonly exhibited the symptoms described above. Since the schedule did not permit further investigation of the problem, EOS was directed to proceed, conducting all operational tests at 5, 10, and 15 micropound thrust levels.

Even with these reduced specifications, difficulties were occasionally encountered during qualification testing and flight acceptance testing. Measures such as increasing the ionizer temperature above 1100°C and using a freshly-cleaned beam collector surface for each test run have helped, but the basic problem remained unexplained.

The desired result of this program was to identify the kind and source of contamination or other mechanism responsible for the degraded performance of some thruster systems, and to devise a method of eliminating the problem.

2.2 TECHNICAL BACKGROUND

Since surface ionization is very sensitive to extremely minute amounts of impurities, only a fraction of a monolayer can change the work function significantly. In many cases, it can be removed only at a very high temperature and extremely low pressure. Porous ionizers have impurities present in the tungsten itself plus those from the cesium propellant, from sputtering and evaporation of accelerator components, neutralizers, and vacuum systems, and from environmental gases and vapors. Potential ionizer contamination sources and types are summarized in Table I.

The porous tungsten ionizers and the braze materials do not appear to be contributors to the alteration of performance since thruster operation is usually flawless at first. Also, impurity contamination has been observed to clean up under chemical cleaning or high temperature flashing but not by prolonged operation (Ref. 1).

Other sources of impurities to which the porous ionizers could have been exposed are sputtering or evaporation of the accelerator electrode material and/or the neutralizer, and sputtering from collectors or other exposed surfaces. Studies of porous tungsten ionizer compatibility

TABLE I

POTENTIAL IONIZER CONTAMINATION SOURCES

Source	Types of Contamination
1. Ionizer	a. Impurities in ionizer material
	b. Diffusion of braze
2. Sputtering and evaporation	a. From neutralizers
	b. From accelerator electrode (usually Cu)
	c. From other electrodes and collectors
	d. Evaporation of braze components, etc., such as Cd, Zn
3. Tank, launch and space environment	a. Residual gas in vacuum tank (O_2, N_2)
	b. Oil vapors in vacuum tank (C)
	c. Space residual gas (O, N, and H)
	d. Launch environment
	e. Vehicle environment (outgassing from other vehicle components such as CLPC)
4. Propellant	a. Initial impurity in commercial cesium
	b. Contamination in storage
	c. Contamination during transfer and in propellant system
	d. Additives

with Cu, Fe, Ti, Ta, and other materials have shown that Cu may be the only material (of those tested) which does not significantly alter ionizer performance. The others tend to clog ionizers and/or increase critical temperatures. Again, these factors were present in all tests and only some thrusters exhibited "roll over."

Effects due to residual gases, including oil vapors, have been discussed extensively in many reports because oxygenation of tungsten is known to increase the work function and ionization efficiency; it is also known to raise the critical temperature. The first reported porous tungsten ionizer evaluation below 10^{-7} torr residual gas pressure (Ref. 2) showed critical temperatures of porous tungsten to be about 180° lower than those obtained at a partial pressure of 10^{-5} torr of oxygen while the neutral fraction about doubled. Residual gas mass spectrometer analysis in the 10^{-9} torr range have indicated H_2, N_2 and traces of H_2O and CH_4, but no O_2 or CO_2 (Ref. 3).

The most comprehensive work on the effect of residual gases upon a porous ionizer was done by Shelton (Ref. 4) concentrating on the simultaneous presence of oxygen and hydrocarbons. In the absence of carbon on the surface, the effect of oxygen on the work function is much more pronounced and a large increase in critical temperature is observed. If the surface is carburized, the presence of oxygen leads to a removal of the carbon as CO. If the carbon is replaced either from the residual hydrocarbon vapors or from within the material, the effect of oxygen is considerably smaller, since it only tries to counterbalance the effect of carbide formation or CO desorption.

Shelton also carburized a porous W ionizer by coating the surface with 0.1 mg/cm^2 carbon lampblack from a sooty illuminating gas flame and heating the ionizer in vacuum. The amount was enough to produce a layer of WC and W_2C 1.6 microns thick. This deposit was probably depleted by diffusion, giving a carbon-rich tungsten instead. The ionizer

was observed to have a faster than normal increase of the neutral fraction with current density, and no observable critical temperature at the high current densities. However, repeated carburization in acetylene (C_2H_2), benzene, and carbon black did not poison the ionizer, and low critical temperatures and low neutral fractions were obtained. An increase in emissivity was observed. Although the carburization experiments are considered inconclusive, they are suggestive of problem sources in oil-pumped vacuum systems.

The other potential sources including the CLPC and the propellant could produce the effects observed. However, all of the potential sources of contamination have been present in all microthruster operations and only some of these have encountered problems.

2.3 PROGRAM APPROACH

The experimental arrangements designed to identify the mechanism which precluded reliable operation of the microthruster system at full thrust (20 μlb) were of two kinds: modification of the vacuum facilities to improve the general cleanliness of the test chamber and modifications to the flight power conditioning and control system (CLPC) to permit measurements of thruster perveance and ionizer critical temperature.

The facilities modification was believed a necessary step toward isolating and/or identifying the source of comtamination. The vacuum chambers were completely disassembled for cleaning, and pumping stations were cleaned and the pump oil replaced. In addition to the normal cleanup, significant alterations included LN_2 traps added to the rough lines of the 1-ft-dia chamber used for wick-wetting and the 2-ft-dia chamber used for systems test. This was to minimize back-streaming of pump oil or vapors to the chamber since they may have contributed to the ionizer problem. Also fabricated was a copper sleeve capable of sliding inside the existing LN_2 shroud for the 2-ft-dia test chamber. This sleeve is more easily removed for cleaning than the existing shroud.

The existing LN_2 shroud consists of a series of baffles which are potential traps for contaminants. The ionizer contaminant may be embedded in these baffles and released by ion bombardment and back-sputtered to the ionizer. The sleeve eliminates this possible source of contamination.

The thermal enclosure used for systems test was also extensively reworked to reduce possible contaminants and provide for easy cleaning and access. A new baffle separating the thruster and CLPC portions of the vacuum chamber was used to improve isolation between these two sections. Provisions for analysis of the residual gas composition in each chamber were also included in the facility modification using a Veeco Residual Gas Analyzer (RGA).

Ionizer investigations required manual variations in the power supplied to the ion engine as follows:

a.	Ionizer heater:	minimum 2.2A at 4.0V
		maximum 2.5A at 4.8V
b.	High voltage:	minimum 1.0 kV V^+, 0.67 kV V^-
		maximum 3.5 kV V^+, 2.33 kV V^-
c.	Vaporizer:	variable from near zero to existing maximum and also capable of normal closed-loop operation.

To meet these requirements temporary modifications to the CLPC were made:

a. The normal ionizer magamp bias was disconnected and a wire was brought out of the CLPC to allow manual variation of ionizer power. To achieve the full range required, the input voltage must be approximately 26 to 27V; so, some of the telemetry channels needed to be recalibrated.

b. A new flight plug was fabricated. Pins 33 and 34, normally jumpered to pins 31 and 32, were connected to an external

wire to allow the HV -24V to be supplied separately. After desensitizing the I^- overload sensing circuit somewhat, the required HV output range could be achieved by varying the voltage to the HV converter.

c. The connection from the vaporizer control circuitry in A14 to the vaporizer magamp was broken and both sides were brought out of the CLPC, together with a ground lead. This allows a choice between normal operation and open-loop, manually controlled vaporizer power.

The program plan was to first determine the thruster subsystem operation in the UHV chamber using laboratory power supplies and compare this operation with full system operation in the 2 x 6 ft chamber. Full system operation was evaluated for three experimental arrangements: the liner sleeve and the baffle separating the ionizer from the CLPC, with both in position; the baffle removed from the 2 x 6 ft chamber but with the liner sleeve in position; and both the baffle and the liner sleeve removed from the 2 x 6 ft chamber. The evaluations of operation were based primarily on measurements of ionizer critical temperatures, the perveance of the thruster subsystem, and the response to both open and closed loop commands. To supplement these data, the kinds and relative amounts of background gas in the chambers were examined using the RGA in the hope of correlating the background gas composition with the thruster performance and with the possible reasons for variations in background gas composition.

2.4 EXPERIMENTAL RESULTS

During the program, five ionizers and three reservoir-valve assemblies were used to provide five thruster subassemblies for testing. The ionizer-reservoir combinations used are listed below in the order of testing, which will also be used for identification purposes.

Subassembly Number	Ionizer (S/N)	Reservoir (S/N)
1	14	03
2	13	03
3	19	02
4	482	03
5	18	08

Of these, only thruster subassemblies No. 1 and No. 5 operated satisfactorily enough in the UHV chamber with laboratory supplies to proceed to full system operation in the 2- x 6-ft chamber.

The first test, subassembly No. 1, went in accordance with the general plan of the program. Operation in the UHV chamber included reservoir wick wetting, vaporizer frequency response determinations, and evaluation of thruster subassembly operation using laboratory power supplies. In all phases of these tests, the thruster functioned flawlessly at thrust levels up to and including 20 μlb. Typical critical temperature and perveance data are shown in Figs. 1 and 2, respectively. Critical temperature measurements, performed over a span of 10 days and at 1000 μA beam current, constantly yielded upper critical temperatures of approximately 1140°C. Lower critical temperatures were ~ 40°C lower. Upper critical temperature is measured with the ionizer temperature increasing; lower critical temperature is measured with the ionizer temperature decreasing.

The perveance of the thruster, also measured, was on the order of 6 nanopervs, calculated from net accelerating potential. The current obtained was not proportional to $V^{3/2}$, and it also indicated that the thruster was perveance-limited at the 3kV V_+ operating voltage.

Attempts to operate the thruster in the UHV chamber using a CLPC located outside the vacuum system were unsuccessful because of voltage drops in the leads and vacuum feedthroughs.

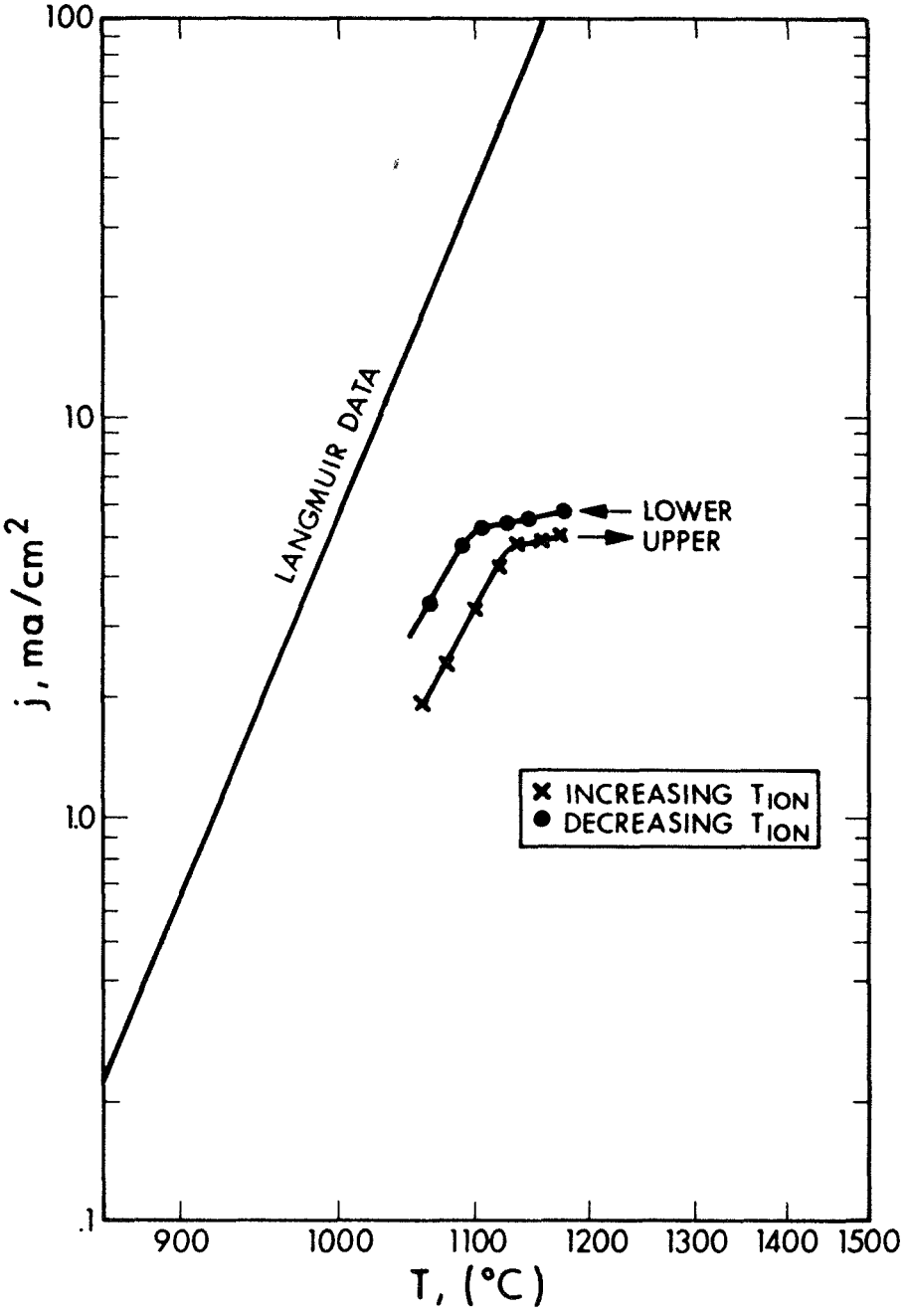

Figure 1. Thruster Subsystem SN 15 Critical Temperature

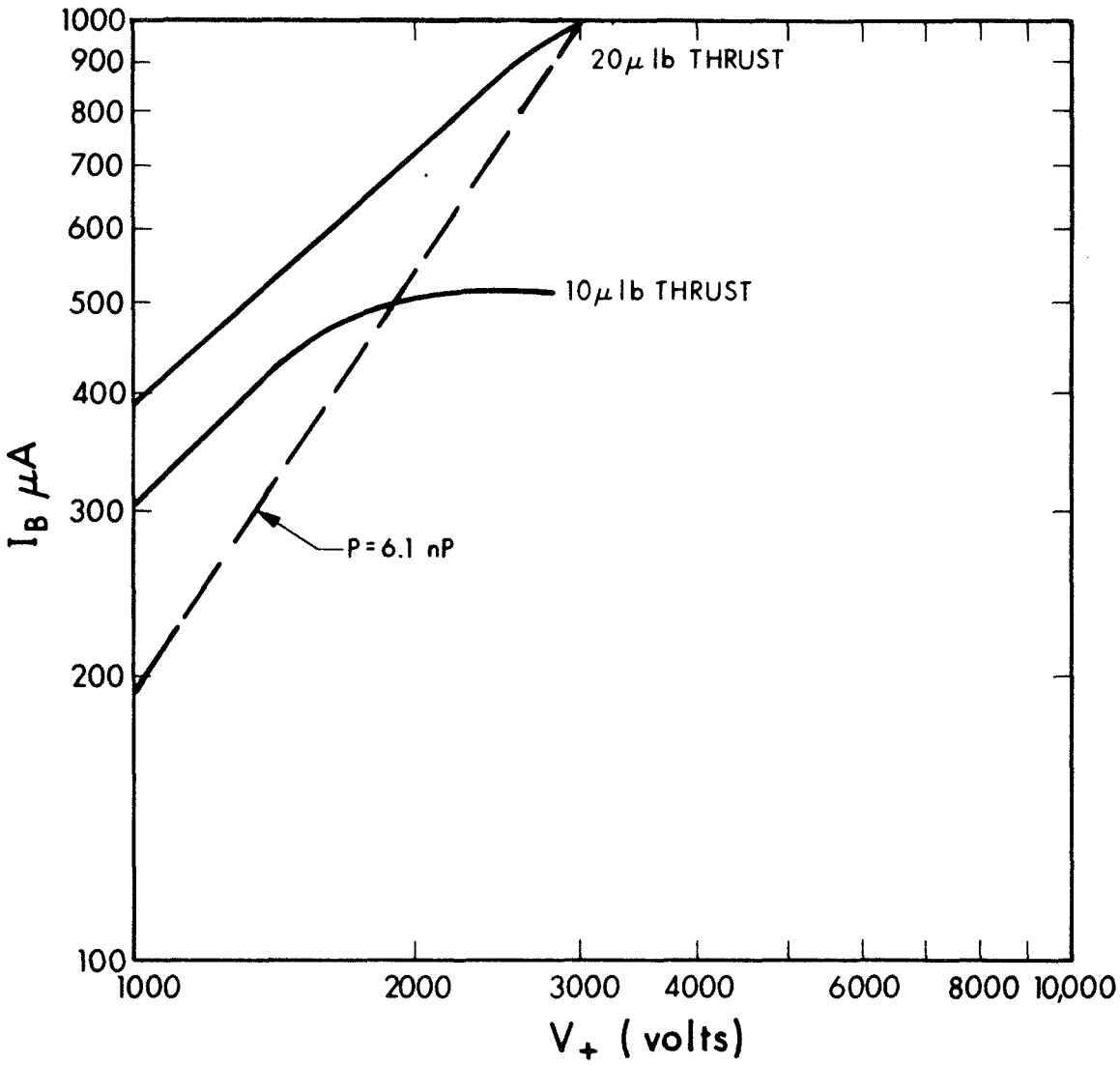

Figure 2. Thruster Subsystem SN 15 Perveance

1016

Testing of subassembly No. 1 was then transfered to the 2- x 6-ft chamber, with the thruster isolated from direct line of sight contamination by the CLPC through the use of baffling and gasketing. The first series of tests were performed with the liner sleeve used to isolate the thruster from the LN_2 shroud in position. For the second series of tests, this liner sleeve was removed and the exhaust beam from the thruster was allowed to impinge upon the shroud.

During the two series of tests, several determinations of critical temperature, perveance, and residual gas composition were made for comparisons between each series of tests and with the earlier data obtained in the 1- x 3-ft system using laboratory supplies.

The operation of the thruster was markedly different during the two series of tests conducted in the 2- x 6-ft facility. During the series with the liner sleeve in position, operation was flawless. There was no difficulty in obtaining 1000 μA beam currents in either open or closed loop vaporizer operation, and there was no hint of ionizer contamination. Critical temperature measurements indicated that the lower critical temperature at 1000 μA (20 μlb) occurred at 1035°C.

During the series without the liner sleeve, there was considerable difficulty in initially attaining a beam current of 1000 μA, and that current level could only be attained in open loop vaporizer operation. Every attempt to go from 15 μlb to 20 μlb in closed loop operation resulted in "roll over." The lower critical temperature at 1000 μA initially occurred at 1100°C, but it gradually decreased to 1070°C as the test continued. In most cases, the upper and lower critical temperatures were quite similar. However, because thermal feedback from the ionizer to the vaporizer affects the cesium vapor flow rate, upper critical temperatures were obtained by extrapolation. This is of little consequence; the principal concern was with lower critical

temperatures since "roll-over" occurs in going from low to high cesium coverage on the ionizer at a given ionizer temperature. This condition is approximated by reducing the ionizer temperature at a fixed cesium supply rate to determine critical temperature.

The change in thruster operation and in critical temperature was accompanied by an alteration in the residual gas composition, and the degraded performance was attributed to an interaction between the ionizer and adsorbed gases sputtered from the previously unexposed LN_2 shroud.

Testing continued after the removal of the baffle which separated the CLPC and the thruster. The copper liner sleeve was reinserted into the LN_2 shroud to preclude further contamination by the shroud while examining the effects of allowing the CLPC to communicate with the thruster.

The operation of the thruster indicated that the ionizer was still contaminated and that performance was slightly degraded from that of the preceding test series. It was very difficult to attain a beam current of 1000 μA since it was necessary to increase the ionizer temperature above normal to reach that level. The accelerator drain currents were erratic, with occasional spikes. Recovery was slower from the high levels that accompany critical temperature determinations than it was in the earlier test series. The critical temperature occurred at about 1100°C, and it remained at that level throughout the test.

The composition of the residual gas in the vacuum system with the baffle removed showed a wider variation with time than in the two previous test series. Initially, with the thruster off, high readings were obtained over the entire range scanned (300 to 12 AMU/e). After running the thruster for a short time, the readings in the 300 to 60 AMU/e range had decreased by about an order of magnitude. The readings in this range dropped below, and remained below, the detection capability

of the residual gas analyzer after the thruster was operated overnight at the 5 μlb thrust level. Typical variations in the 60 to 12 AMU/e range are illustrated in Table II which also includes the data from the two preceding test series for comparative purposes. In the previous test series, where contamination was inferred from the way the thruster operated, the readings for values of AMU/e of 28 (CO or N_2), 32 (O_2) and 14 (CH_2 or N) observed when the LN_2 shroud was exposed to the ion beam indicated that oxygen and hydrocarbon vapors were being desorbed or sputtered from the liner and were reacting with the ionizer to give rise to the increased readings of CO. The further degradation of thruster performance accompanied by increases in the residual gas readings was in line with this hypothesis; i.e., oxygen and hydrocarbon vapors were reacting with the ionizer and producing the deleterious effect observable as "roll-over."

To substantiate these findings, subassembly No. 2 was installed in the UHV chamber for testing using laboratory power supplies. Because of experimental difficulties, including a vacuum system leak in the UHV 1- x 3-ft vacuum facility, the results obtained may not be completely pertinent to the type of contamination observed in flight qualification testing. Ionizer contamination effects were observed in tests with subassembly No. 2, and it was decided that both the vacuum and the feed system (reservoir S/N 03) could be sources of the contamination. To verify these conclusions, another feed system (reservoir S/N 08) was loaded and, as subassembly No. 3, it was installed in the 2- x 6-ft vacuum system. Attempts to wet the porous nickel wick failed. Consequently, a third ionizer (S/N 482) and the suspect feed system (reservoir S/N 03) were installed as subassembly No. 4 in the 2- x 6-ft vacuum system in a further attempt to establish the source of contamination. In this test, ionizer contamination effects were observed almost immediately. They indicated that the feed system was the principal source of contamination for ionizers S/N 13 and 482.

TABLE II

SUMMARY: RGA DETERMINATIONS

Test Facility	2- x 6-ft (With Liner Insert; Baffle Removed)			2- x 6-ft (Without Liner Insert; Baffle in Place)		2- x 6-ft (With Liner Insert; Baffle in Place)	
Test Series	3			2		1	
AMU/e	Initial	After 1.5 hr	> 15 hr	High	Low	High	Low
44	10.5	5	0.1	1.3	0.35	0.34	0.13
32	2.5	1.3	0.3	2.8	2.0	0.25	0.16
28	21.0	22.0	8.8	48.0	28.0	2.3	1.1
18	61.0	14.0	0.87	2.7	1.0	16.0	5.6
17	16.5	4.5	0.26	0.86	0.45	4.8	1.7
16	7.5	3.7	0.39	6.4	1.25	1.0	0.5
15	3.7	1.7	0.24	4.4	0.35	0.27	0.04
14	4.6	3.5	1.5	7.2	5.0	0.36	0.25
13	0.69	0.33	0.03	0.25	0.05	0.07	NO
12	2.6	2.0	0.05	0.35	0.1	0.18	0.06

The last available ionizer assembly and a newly loaded reservoir assembly were used in subassembly No. 5. Operation in the UHV chamber was flawless during wick wetting, vaporizer frequency response determinations, and the evaluation of thruster performance using laboratory power supplies. The operation was very similar to that of subassembly No. 1, including an identical upper critical temperature of $\sim 1140^{\circ}C$.

Testing of subassembly No. 5 was then transferred to the 2- x 6-ft chamber after mating with the CLPC. The CLPC had been modified back to the original flight version as required for testing the new modules; therefore, the provisions for varying the ionizer temperature, varying V_+, and open or closed loop vaporizer operation were lost. It was therefore necessary to operate the thruster as a flight unit. In addition, the test sequence was altered from that used with subassembly No. 1. Since it was felt that the LN_2 shroud was the most probable source of contamination, the baffle separating the ionizer and the CLPC was removed prior to removal of the liner sleeve. During all testing sequences, the thruster system operation was near perfect. With both the liner sleeve and the baffle removed, there were occasional oscillations in the vaporizer current with corresponding oscillations in beam current and occasional increases in accelerator drain current. In general, however, the thruster operated satisfactorily even with the LN_2 shroud exposed to the beam. The residual gas composition indicated that significant quantities of hydrocarbon vapors and oxygen were present and were reacting with the ionizer to increase the amount of CO (AMU/e of 28) present in the chamber; however, the ionizer was not contaminated. In a deliberate attempt to contaminate the ionizer, hydrocarbon vapor from the rough pump was caused to backstream into the chamber and the thruster was operated in this "contaminant rich" environment. If anything, the operation was superior to that observed previously even though the quantities of hydrocarbon vapor were much larger than in any of the preceding test series. The CO peak was off scale (> 100) as a result of the hydrocarbon-oxygen interaction with the ionizer and was positively identified in this test.

2.5 SUMMARY OF RESULTS

During this program, potential kinds and sources of ionizer contamination have been considered and experiments designed to evaluate the presence of contaminants have been performed. Contamination or characteristics consistent with those expected if ionizers are contaminated were observed. There is evidence from one test that the vacuum chamber environment can influence thruster operation; this evidence is refuted by evidence from another test. There is also evidence from two tests that the reservoir assembly was responsible for observed contamination even though another (prior) series of tests, which used the same reservoir assembly, was initially flawless.

In summation, no conclusive results were obtained that identify the contamination or source of contamination observed in flight qualification testing of ATS microthrusters.

SECTION 3

IONIZER PROTECTIVE COATINGS

3.1 COATING BENEFITS

The project endeavors to find an ionizer coating material for prelaunch thruster protection. A twofold goal is anticipated. First, the ionizer button itself will be protected from contamination due to airborne particles. It is believed that the proximity of the spacecraft launch facilities to the ocean subjects the thrusters to high concentrations of airborne salts. These will be kept from clogging the ionizer by a suitable coating. Second, since the thrusters remain on the earth effectively in storage after the feed tube wick has been wetted, sealing of the ionizer will prevent contamination of any cesium left in the feed tube between the vaporizer and the ionizer. Obviously, such protection will increase the level of confidence in thruster systems which have endured lengthy storage periods on the earth prior to launch.

3.2 COATING REQUIREMENTS AND SELECTION OF COATINGS

Selection of a suitable coating necessitates consideration of performance requirements as well as manufacturing and assembly processes. The period when the risk of contamination becomes great is that period between final acceptance testing at the supplier and launching out of the atmosphere.

Therefore, a coating is required which can be applied to the thruster after operational acceptance testing. The coating must then remain stable in air for a period of one year at temperatures encountered during storage, flight preparation, and launching. The coating must also have a reasonable stability in vacuum so that it will remain intact in orbit. Then, it will be possible to protect the thruster from the effects of outgassing of the spacecraft. The specified storage temperature for the thruster is 100°F. To provide a margin of safety, the investigation was confined to coating materials with minimum indefinite period service temperatures in air greater than 115°F.

The upper service temperature specification must be chosen as low as possible to ensure that the coating material will not interfere with the operation of the thruster. The coating material must evaporate, leaving no residue as the ionizer is heated the first time after application of the coating. It takes about 5 minutes for the thruster to reach 1000°C. At this temperature it is feared any coating remaining upon the ionizer would effect it detrimentally. Keeping these temperature constraints in mind, it was decided to investigate the materials for protective coatings which are given in Table III.

Metallic cadmium was chosen for its low melting point, high vapor pressure, and inertness with respect to tungsten. The various plastic materials, which were chosen from a list of modern plastics, were selected solely on the basis of having the lowest service temperatures above 115°F.

The biphenyl was chosen because of successful application to the protective sealing of resistojet nozzles.

TABLE III

IONIZER COATINGS TO BE TESTED

Trade Name	Supplier	Formula	Service Temperature
Adiprene L100	DuPont	Urethane polymer (NH_2 $COOC_2H_5$)	190 to 250°F
Biphenyl	GSFC		melts at 158°F
Cascamite 151	Borden	Urea formaldehyde	170°F
Dimethylol Urea	Glyco	Urea formaldehyde (H OCH_2-NHCONH-CH_2OH)	170°F
Ethyl Cellulose, N-50 49. Hz	Herculese	49% by wt ethoxyl (-OC_2H_5) substituted into anhydroglucose (q.v.)	115 to 185°F
Styron 475	Dow	(Polystyrene, φ-CH:CH_2-; + 4 to 6% butadiene (CH_2:C:$CHCH_3$)	140 to 175°F
Styron 666 (polystyrene)	Dow	Polystyrene	150 to 170°F
Tybrene 213 (Acrylonitrile-Butadiene-Styrene, ABS)	Dow	Acrylonitrile butadiene styrene	140 to 200°F
Vinyl-Formal Molding Compound	Union Carbide	φ-CH:CH_2- X CH_2O	120 to 150°F
Metallic Cadmium	Research Organic	Cd	melts at 608°F

3.3 APPLICATION OF COATINGS TO IONIZERS

Application of the plastic materials to the ionizer was then considered. Just as it was necessary to protect the ionizer from degradation because of the temperature requirements, it was also necessary to determine that the application of the plastics would not leave harmful residues on an ionizer or damage it in other ways. The urethane, urea formaldehyde, and vinyl formal molding compounds required plasticizing processes that were felt to be harmful. Heat curing was one method, but this was felt to be unwise as temperature control would be difficult on the ionizer button. Also, these materials give off formaldehyde residues upon curing and the effect of such chemicals upon the tungsten ionizer at elevated temperatures is naturally to be suspected.

Chemical precipitation was the other method for setting these plastics. Ammonium chloride salts and precipitation from a hydrochloric acid solution is involved. Chlorides of tungsten might form in the process and these would probably harm the ionizer. Thus, the urethane, urea formaldehyde and vinyl formal molding compounds were rejected due to expected difficulties in application to the ionizer button.

The plastic materials considered for further investigation were soluble in organic solvents, which were least likely to harm the ionizer. It was planned from the outset to vapor-deposit the cadmium, so the question of contamination by solvents did not arise.

3.4 SEALING AND EVAPORATION TESTS

Having decided which materials met the temperature requirements and application considerations, tests were devised to check acceptability in practice. This implied testing ease of application, ability to seal an ionizer, short term film stability in vacuum, and evaporation without

trace during heating of the tungsten. It was found that the plastic materials dissolved easily in the ratio of 100 milligrams of plastic to one milliliter of solvent.

For application and temperature range tests the various materials were applied to flat porous tungsten disks or "buttons" of a size similar to the spherical ionizers (1 mm thick by 5 mm in diameter). The buttons were first tested for permeability to nitrogen gas, as is done with normal ionizers. Then, they were photographed and coated with their particular plastic sealing material. After drying in air, the buttons were again permeability checked to determine if sealing of the surface had been effected. Table IV, "Gas Permeability of Tungsten Buttons," shows the data. Three materials, Styron 475 and 666 and cadmium were perfect sealants; Tybrene and biphenyl were effective to a lesser degree.

At this stage in the proceedings the biphenyl compound was found to be unacceptable. It evaporated completely within 24 hours after being coated onto a tungsten button. The effect was checked numerous times after recoating to ensure the correctness of the result. It is assumed that the effect would be accelerated in a vacuum. Success with this material in another application was probably due to the fact that it was used to seal the inside of a small-diameter tube. Such a configuration would naturally tend to hamper sublimation of the material.

The plastic coating materials found to be acceptable for ease of coating and short-term stability in the atmosphere were ethyl cellulose (soluble in toluene), Styron 475U (polystyrene with 4 to 6% butadiene), Styron 666U (polystyrene), and Tybrene 213 (acrylonitrile, butadiene, styrene polymer). The last three materials are soluble in methyl-ethyl-ketone.

The buttons were photographed after checking the gas permeability when coated with the acceptable materials. Next, they were heated on a flat

TABLE IV

GAS PERMEABILITY OF TUNGSTEN BUTTONS*

Coating Material	Gas Flow Times: Uncoated Button	Coated** Button	Coated and Heated Button	Time*** Change
Styron 475	25.6 sec	impermeable	25.6 sec	none
Styron 666	29.0 sec	impermeable	27.3 sec	-5.8%
Tybrene 213	30.0	216	not measured	
Ethyl cellulose	38.2	218.3	39.6	+3.7%
Metallic cadmium	17.9	impermeable	not measured	

*Measured as time for 10 cc dry N_2 gas at 10 psig to pass through the button. Lower times mean higher permeability and vice versa.
**High times indicate good sealing properties.
***Change in time between an uncoated button and a button that has been coated and heated.

heater plate in the vacuum chamber. The button temperature was monitored with an optical pyrometer which indicated a temperature rise to 900°C in 10 minutes. In all cases the coating materials evaporated before the buttons had reached 700°C (this was the lower reading limit of the pyrometer). Evaporation was visually detected through the pyrometer telescope by watching the film disappear from the button.

After the heating test, the buttons were photographed again and examined for evidence of any superficial changes to the plastic materials. The two styrene plastics and the acrylonitrile-butadiene-styrene (Tybrene 213) appeared unchanged. However, there were little brown spots of about 1/2 mm diameter on the button that had been coated with ethyl cellulose. Not wishing to become involved in the investigation of the reason for these spots, and assuming that they implied some modification of the tungsten surface, it was decided to reject ethyl cellulose as an unfit coating. It was found that the other coatings had evaporated completely and did not lower the gas permeability of the buttons from their precoating values as indicated in Table IV.

The coating and heatup tests resulted in a choice of three plastic coating materials which met the initial thermal and mechanical considerations.

The cadmium was applied to the button by vapor deposition. Two copper arms held a piece of cadmium foil 1 in. long at a distance of 1 in. from the button to be coated. A mask was used to keep cadmium off the rest of the ionizer assembly. Figure 3a shows the assembly and Fig. 3b shows the shape of the wire used. Typically, evaporation started at 3.5 to 4A and 0.160V drop in the wire. Evaporation lasted for seven minutes on the ionizer that was tested. There was a 0.160V drop in the wire and the current decreased from 4.5 to 2.5A; at this point the wire fuzed open. A test deposition was made on a weighted piece of foil. It was found that 50 micrograms of cadmium accumulated in two minutes at 3.8A and 0.140 to 0.170V. Thus, we estimate, by multiplication of the time factor, that approximately 175 micrograms were plated onto the ionizer used in the performance tests. A flat button was coated and the cadmium provided an effective seal. Since some experience with cadmium had been accumulated on previous programs, the evaporation test was deleted and preparations were made for thruster tests.

3.5 PERFORMANCE TESTS

The next logical step in the process involved looking for performance changes which might occur in thrusters that had been coated. For this purpose it was merely necessary to fabricate or obtain a sufficient quantity of new ionizers to test each of the coating materials; the three plastic coatings and the metallic cadmium were available. Four separate tests were conducted using complete thruster subsystems consisting of a feed system, ionizer, accelerator electrode assembly, and neutralizer assembly. It could then be determined if the coatings impaired the operation of the ionizer or the neutralizers. Also, whether

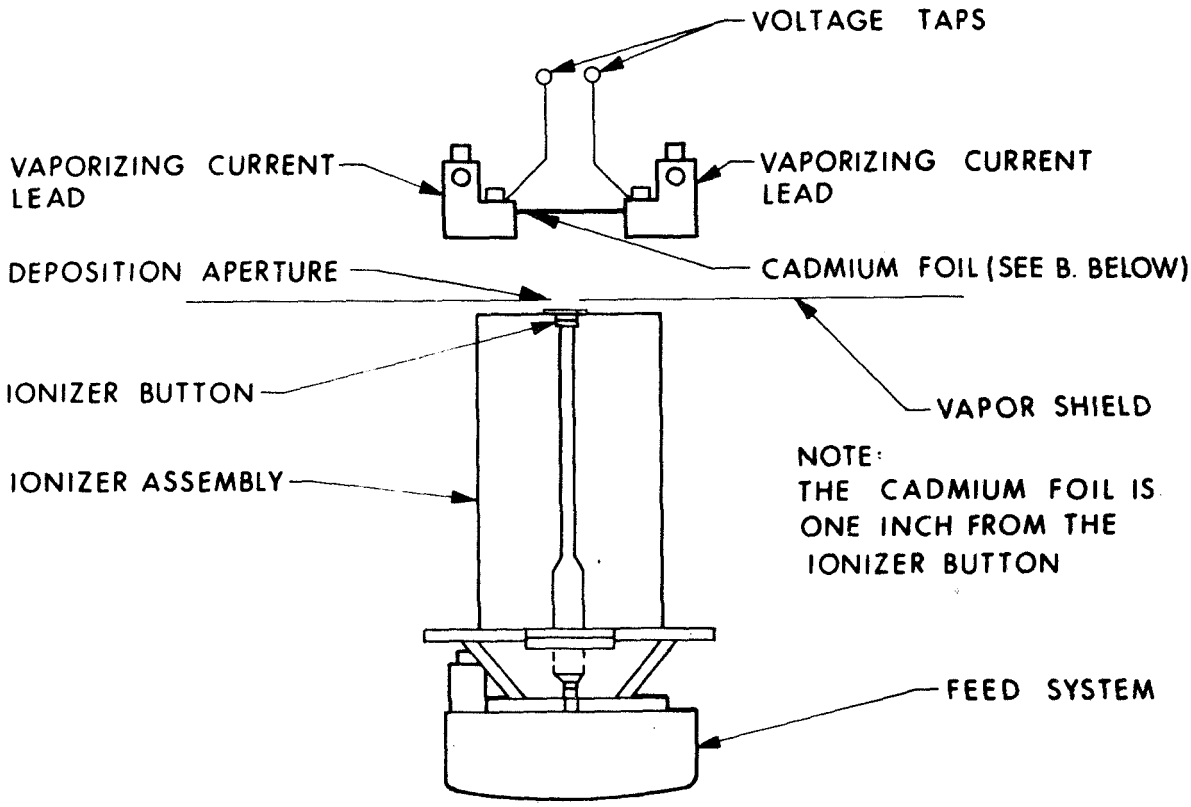

A. CADMIUM DEPOSITION APPARATUS, SIDE VIEW

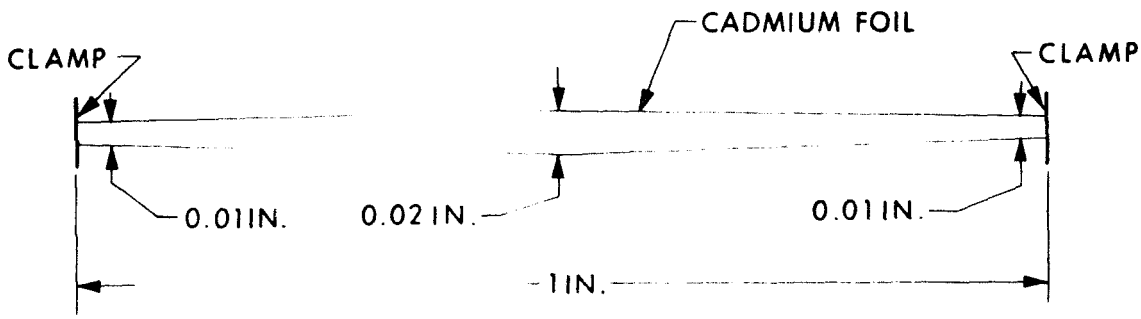

VIEW LOOKING DOWN TOWARD IONIZER BUTTON

THE SIDE CROSS SECTION IS A UNIFORM THICKNESS OF 0.010 IN. (STOCK)

B. CADMIUM FOIL SHAPE

Figure 3. Cadmium Deposition Apparatus

or not the evaporation of the coating effected the accelerator electrode in such a way as to cause high currents to flow to it (high drain condition) could be determined.

Two types of ionizer tests were made before and after coating with the various materials. First, the thruster was run to see if it would operate properly at a 1000-μA beam, the design maximum. Secondly, the critical temperature of the ionizer at this beam level was determined. The critical temperature test consists of establishing a stable cesium flowrate and then measuring the ion beam emitted at decreasing and increasing ionizer temperatures.

The tests are run by lowering the ionizer temperature from the 1160 to 1180°C level until the point is reached at which the rate of beam current drop off with temperature becomes precipitous.

At this point, the ionizer is reheated and the increase in beam is noted. Critical temperatures are taken to be the points at which tangent lines to the level curve of log beam versus ionizer temperature intersects the line tangent to the data on the sharply decreasing leg. Figure 4 "Critical Temperature Measurement," shows such a curve with the points taken as the critical temperatures marked upon it.

The following paragraphs present the results of the tests conducted with the four coating materials.

Styron 475: An ionizer test assembly was given a coating of Styron 475. The critical temperatures (upper and lower) before coating were both 980°C at 1000μA ion beam. After coating there were high accelerator currents (~ 100 μA) at the 1000 μA operating point. At 850 μA ion beam, the critical temperatures were approximately 1000°C, although the high accelerator currents hindered the measurements. Styron 475 was deemed unacceptable because of these high accelerator currents.

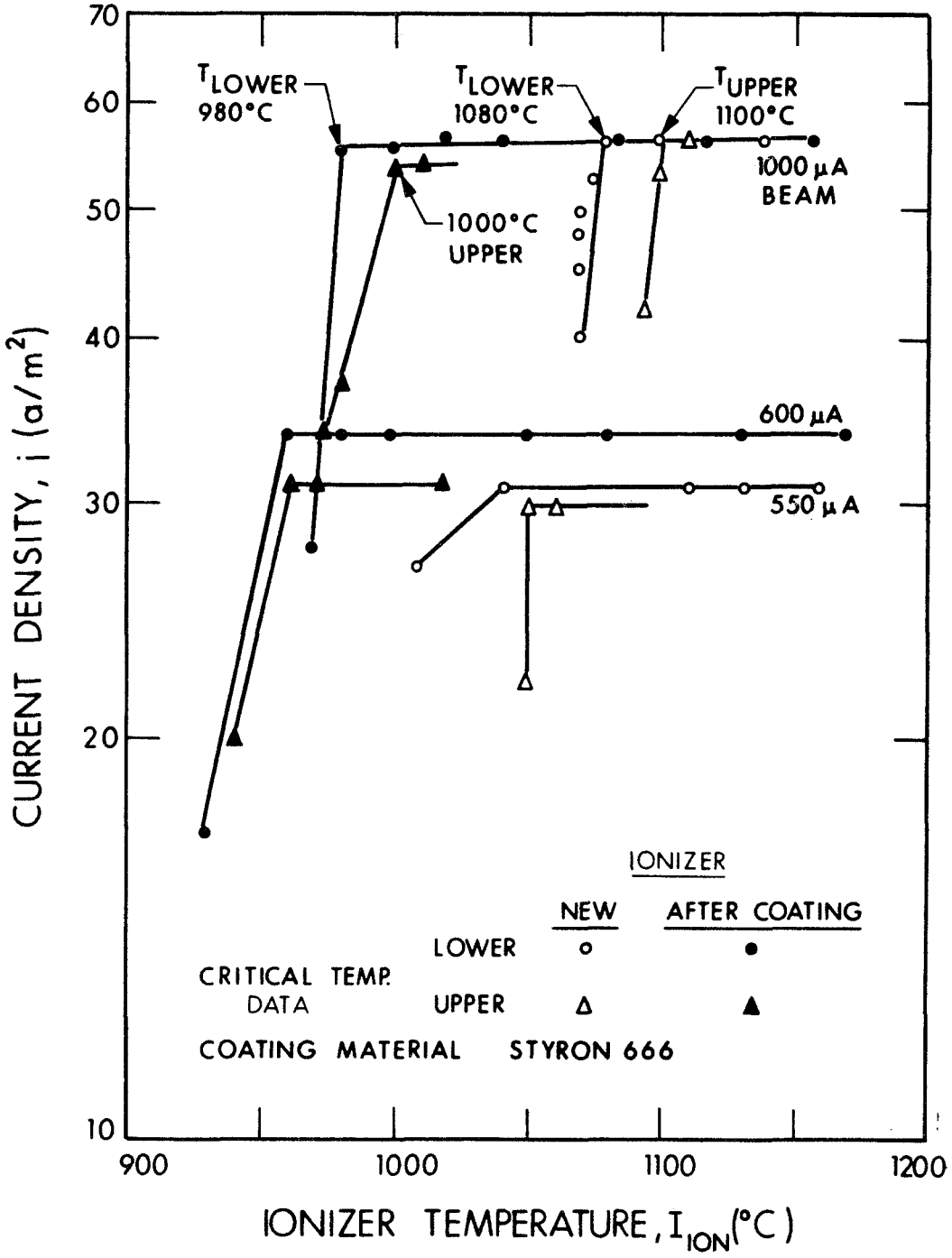

Figure 4. Critical Temperature Measurement

Styron 666: The next ionizer assembly was operated uncoated for calibration. After coating with Styron 666 styrene plastic, operation was successful. Measurements of critical temperature indicated no increase due to the plastic material. Table V presents before and after critical temperature values. In addition, neutralizer performance was not affected by the plastic. This platic is deemed acceptable.

Tybrene 213: This plastic was also tested on a new ionizer and caused extremely high accelerator currents at 1000 μA ion beam. The ionizer had operated perfectly before coating. Performance was so poor that critical temperature could not be measured after coating. The plastic is deemed unacceptable because of the high accelerator currents.

TABLE V

CRITICAL TEMPERATURE CHANGES

a. Effect of "Styron 666" on Critical Temperature

Beam Current	New Ionizer	Coated	
1000 μA	1100°C	1000°C	Upper $T_{Critical}$
	1080	980	Lower $T_{Critical}$
550 to 600*	1050	960	Upper $T_{Critical}$
	1040	960	Lower $T_{Critical}$

b. Effect of Metallic Cadmium on Critical Temperature

1000 μA	1100	1105	Upper $T_{Critical}$
	1082	1040	Lower $T_{Critical}$

*New Ionizer tested at 550 μA, at 600 μA after coating.

Metallic Cadmium: An ionizer assembly was operated uncoated for calibration. After coating with metallic cadmium by vapor deposition in vacuo, operation was successful. Measurements indicated a slight decrease in critical temperature. In addition, neutralizer performance was slightly improved. Table V presents the before and after critical temperature data.

3.6 1000-HOUR EVALUATION TEST

Four materials were tested and found acceptable under initial conditions; two of them are acceptable as evidenced by thruster performance. The next and final step in the test program was a determination of long term acceptability of the coating material. This could be determined only by testing an ionizer, which had undergone coating, for a period of time (1000 hours). Due to the timing involved in setting up a 1000-hour test during the contract period, the Styron 666 was chosen as the coating material for such a test. The vapor deposition apparatus for the cadmium and receipt of the cadmium from the supplier were delayed; consequently, tests were not completed in time to allow use of cadmium for the 1000-hour run. It seems, from the initial tests, that cadmium would perform well also.

A new ionizer (S/N 34) was assembled with a valve operated feed system (S/N 12-9). Operation of the thruster was verified at 1 mA beam level with no accelerator current evident; the critical temperature was measured as 1010°C.

After the initial test run, the thruster electrodes were disassembled and cleaned. A half drop of Styron 666 dissolved in methyl-ethyl-ketone (100 grams per milliliter) was allowed to spread over the ionizer button surface. Two hours were allowed for drying, the thruster was reassembled and placed in a 1 x 3 ft vacuum system.

The test run was started at 12:05 on 10 April 1969. Successful operation at 1000 μA beam was experienced for 71 hours, with accelerator currents averaging 16 μA. After this time drains started to increase to a level of 40 μA. Deflection of 600V in the +y direction lowered accelerator currents to 20 μA; drain current was predominantly from one accelerator electrode segment.

After 173 total test hours, the I^- had increased to 80 μA with full deflection as above. It was decided to operate at a reduced beam level. Upon lowering to 390 μA, the I^- current dropped to 11 μA. After 260 test hours, the drain current had risen to 28 μA. The deflection was turned off, and the drain current rose only to 30 μA. The beam was raised to 490 μA after 293 test hours. A 600-V deflection in the minus x direction lowered a 32-μA, I^- current to 24 μA, indicating principal drains had changed from one deflection segment to another. Deflected operation was performed through the remainder of April. The beam current then was 500 μA, with 25 μA of I^-; the test time was 492 hours. No further deterioration was seen in performance. Similar drain current behavior has been observed on several other thrusters and it is believed that the styrene is not the cause of this condition.

On 16 May there were 23 μA of I^- current with the deflection still on. The beam was raised to 1050 μA and the I^- increased only to 30 μA. The deflection was switched off and the I^- dropped back to 22 μA. Most of this was still going through the plus x electrode. However, it should be noted that this represents an improvement over the 80 μA total I^- seen after 173 hours. The critical temperature was measured and found to be 1000°C (upper and lower about the same), which compares well with the 1010°C measured before coating of the ionizer. The thruster was operating at 1000 μA beam and 25 μA I^- on 17 May. It was shut off at 1740 hours PDT, after having accumulated 893 hours and 35 minutes run time since commencement of the test. The power supply console was needed for other tests on the program, and the off cycle offered an opportunity to see if the thruster had kept its restart capability.

On 3 June 1969 the thruster was easily and successfully restarted and ran successfully at 1000 μA beam. The I^- was initially 35 μA, but this decreased to between 10 and 20 μA for the duration of the test. As before, half the total I^- was concentrated in the plus x electrode. This could have been due to contamination of the electrode or the insulator by cesium compounds, or slight misalignment of the electrode because of temperature effects. As was mentioned previously high I^- currents have been noticed on other thrusters and it should not be concluded that these are due to the coating material.

The test was terminated on 9 June 1969 after accumulating a total run time of 1039.8 hours, of which 259.8 hours were at full thrust (1000 μA). Table VI, "1000-Hour Test Results," summarizes the operation of the plastic-coated thruster. The off time from 17 May to 3 June is not reckoned into the test time calculations.

3.7 SUMMARY

Various coating materials were chosen on the basis of service temperature ranges. They were then investigated as to acceptability of application methods. At this point, urethane, urea formaldehyde, and vinyl formal molding compound were deemed unacceptable due to expected procedures or results of application. The usable materials were given coating and evaporation tests to determine their efficiency as sealants and their compatibility with heating porous tungsten. Biphenyl was rejected at this stage because it evaporated in air, and ethyl cellulose was rejected because it caused the ionizer to spot. Tests on the effects of the materials upon operation of ionizers were then conducted. Styron 475 plastic was rejected as was Tybrene 213 because they interfered with ionization and caused high I^- currents. Styron 666 and metallic cadmium remained as acceptable materials. The Styron was tested for 1000 hours and it did not appear to impair thruster operation. The cadmium

TABLE VI

1000-HOUR TEST RESULTS

Thrust μlb			0	10			15			20			
Time Thru		Notes	Idle	No Defl	10° Defl	Total	No Defl	10° Defl	Total	No Defl	10° Defl	Total	Total Test Time
Date	Time		Hrs	Hrs	Hrs	Hrs	Hrs			Hrs			Hrs
4-10-69	1205	Start											0
4-17-69	1740		2.1	0	0	0	0	80.5	80.5	69.0	22.0	91.0	173.6
5-17-69	1740	Off	2.1	32.2	663.1	695.3	0	80.5	80.5	93.7	22.0	115.7	893.6
6-3-69	1452	Restart	2.1	32.2	663.1	695.3	0	80.5	80.5	93.7	22.0	115.7	893.6
6-9-69	1716	End	4.3	32.2	663.1	695.3	0	80.5	80.5	237.7	22.0	259.7	1039.8

coating could not be so tested for lack of time. Table VII, "Test Results," gives the results of the various tests performed on the coating materials.

The acceptable plastic material was characterized by the manufacturer as polystyrene, Styron 666. Styron 475 contained butadiene rubber (4 to 6%) and was not acceptable, although it was basically polystyrene. The Styron 666 is a general purpose polystyrene which can be used for containers, toys, housewares, and the like. It is manufactured in bulk quantities. The manufacturer stated that there was no available data on vapor pressure or life time in a vacuum environment. There was no apparent degradation over a span of a few hours in vacuum in the tests, however.

Cadmium has an evaporation rate of less than 1.0×10^{-9} gram per second per square centimeter at a temperature of $38^{\circ}C$ ($100^{\circ}F$). Since the ionizer button area is approximately 0.18 square centimeter, it is necessary to supply cadmium for an evaporation rate of less than 2×10^{-10} gram per second. The initial deposition during this contract was approximately 175×10^{-6} gram, which would take more than $8.7 \times 10^{+5}$ seconds or 10 days to evaporate. This could be extended by repeating the vapor deposition several times.

Since the cadmium layer deposited was insufficient to protect the ionizer for a period of several hundred days, the compatibility results reported must be considered preliminary. Ionizer compatibility is fairly well established since only a few monolayers of an incompatible substance would be required to affect ionizer performance. Compatibility with the accelerating electrode is less well established since the details of the formation of low work function compounds are not well understood.

TABLE VII

TEST RESULTS

Plastics	Application to Button	Evaporation From Heating Button	Effect on Thruster Operation	1000-hour Thruster Test Run
Adiprene L100	Not feasible			
Biphenyl	Evaporates cold in atmosphere			
Cascamite 151	Not feasible			
Dimethylol urea	Not feasible			
Ethyl cellulose	X	Leaves spots		
Styron 475	X	X	High I^-	
Styron 666	X	X	X	X OK
Tybrene 213	X	Inconclusive	High I^-	
Vinyl formal molding compound	Not feasible			
Metallic cadmium	X	X	X	

X denotes test completed acceptably.

SECTION 4

CLPC DESIGN MODIFICATION

The circuit investigation was limited to the most significant potential problem areas. The specific goal of the investigation was to develop circuitry with the following objectives:

a. Reduce the sensitivity of the thrust level and deflection circuits to transients on the power and command leads.

b. Ensure that the thrust status counter circuit is in the correct state when the system is turned on.

c. Increase the stability and repeatability of the high voltage overload circuits.

In addition, an analysis was to be made of the vaporizer control circuitry as part of an overall beam control stability investigation.

The poor transient immunity of the command interface circuits was also recognized as a problem, but was considered to be relatively easy to correct in future flight systems. By limiting the present investigation to the problem areas listed above, only four modules need be constructed for a system test. If the thrust level adjust and deflection adjust command circuits were included, an additional three modules would have to be built. It was decided that the effort involved was not justified.

4.1 FLIP-FLIP TRANSIENT IMMUNITY

Since the beam deflection counters and thrust level control counters are identical, the investigation was simplified somewhat. A breadboard of the thrust level select binary counters was constructed and used to test proposed modifications of the circuit for immunity to transients

on the command and +12V lines, referred to local ground. During these tests, the breadboard incorporated a digital-to-analog converter circuit which replaced the original resistive dividers which were the cause of the heavy loading on the flip-flops. This new circuit is referred to here as the Mk II circuit, and is shown in Fig. 5.

Modifications to the flip-flops which were tried were the addition of 820K resistors to provide a trigger threshold, as recommended by Planning Research Corporation, and the increase in value of the 330 ρF switching capacitors to 0.003μF, to discriminate against narrow transients. The voltage required to trigger the flip-flops for positive rectangular pulses of different pulse widths on the command line is shown in Table VIII for the modified and unmodified circuits. Negative pulses on the command line of only 0.5V were found to cause triggering even when they were very narrow. A diode network in the command line was tried; it proved to be very effective and was incorporated.

TABLE VIII

LEVELS REQUIRED TO TRIGGER FLIP-FLOPS FOR POSITIVE RECTANGULAR PULSES ON COMMAND LINE

Pulse Width μsec	Original Circuit C=330ρF 820K out Volts	C=330ρF 820K in Volts	C=0.033μF 820K out Volts	C=0.033μF 820K in Volts
10	1.6	4.8	0.20	4.1
5	1.55	4.8	0.35	5.9
2	1.55	4.8	0.90	11.8
1	1.55	4.8	2.20	25
0.5	1.50	4.8	4.05	44
0.2	1.60	5.0	10.2	
0.1	2.20	6.3	22.5	
0.05	3.4	9.4	43	
0.02	8.4	19.5		
0.01	15	33		
0.005	29			

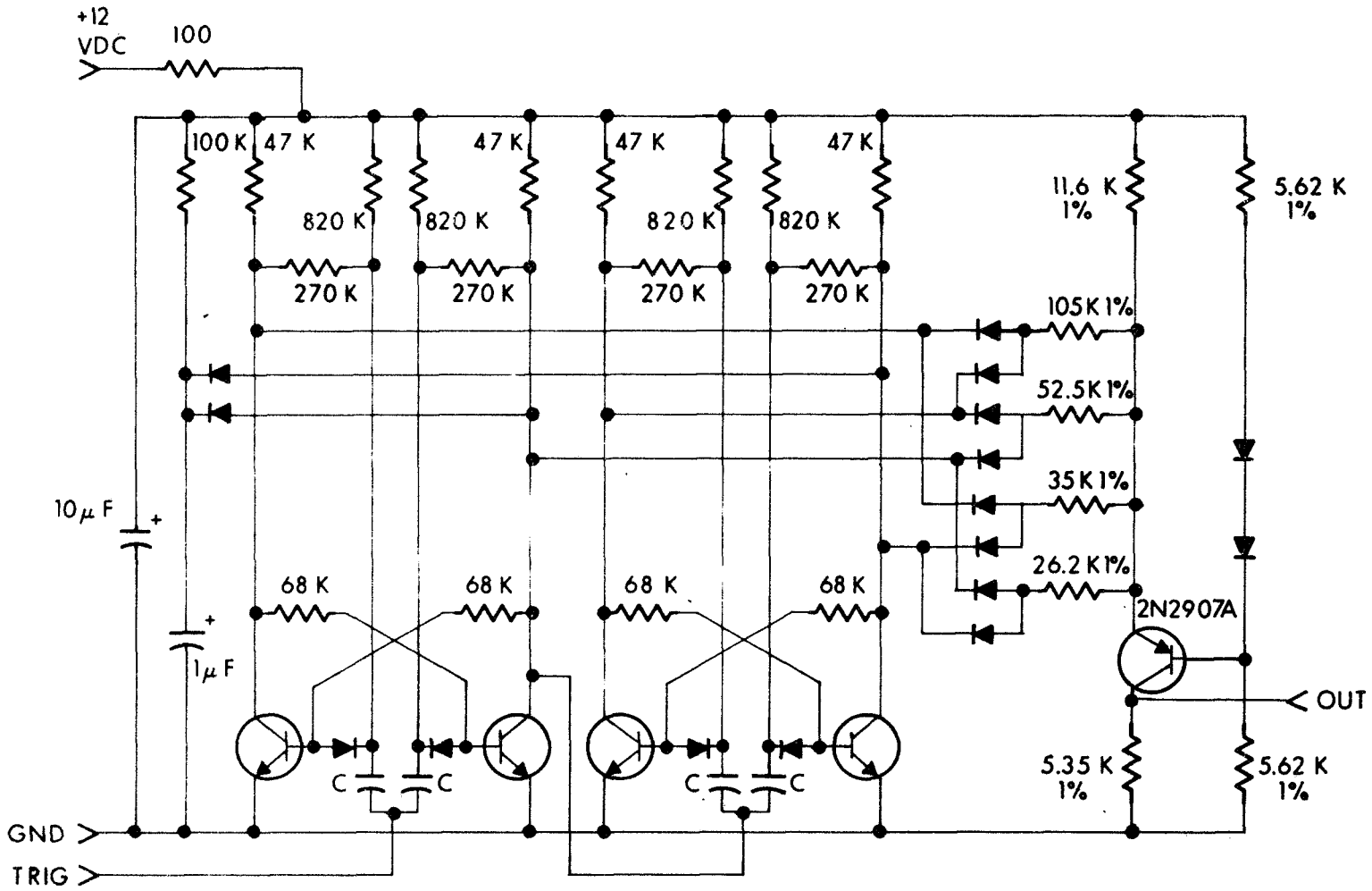

Figure 5. Turn-On Steering Circuit

Fast rise-time transients with exponential decay time constants of 8 μsec and 100 μsec were impressed on the +12V supply line. Positive transients had no effect on the state of the flip-flops even with amplitudes of 50V. Negative transients would cause the flip-flops to transfer when the amplitude was 3.6V or more without the 820K resistors, or 7.5V or more with the 820K resistors. These figures are for the 100 μsec transients; the circuit was slightly less sensitive to the narrower ones. This test was made with the 0.033 μF switching capacitors, and of course the normal 100 ohm, 10 μF filter network was disconnected. With this network connected, no transients of 7.5V are expected.

No tests were made of immunity to transients on the output line, but due to the inherent isolation of the collector circuit the trigger level here should be in excess of 6V positive (+) and much higher negative.

To improve the reliability of the turn-on steering circuit, the 0.1 μF capacitors in A12 were replaced by one 1.0 μF capacitor (Fig. 5). In testing the circuit to ensure proper turn-on operation, it was noted that under certain conditions both flip-flops would come on with all transistors in an "on" state. When this occurred, the collector voltage was 1.1V and the base voltage was 0.55V. Analysis showed that with the lighter loading of the new D-to-A circuit, the voltage across the 69.8K base resistors supplied enough current to drive the transistors near saturation.

This phenomenon occurred only when the 10 μF filter capacitor was connected, the 100 ohm decoupling resistor was bypassed, and the supply connected suddenly after having been disconnected long enough to allow the voltage on the 10 μF to decay to not less than 250 mV. This would seem to indicate that the problem is not too serious. Nevertheless, the existence of such a mode was disturbing. Possible solutions were to increase the 69.8K resistors to a larger value, shunt the base junction with a resistor, or both. However, the basic problem appeared to be due to the relatively poor saturation characteristics of the 2N910. It was decided simply to replace them with the 2N2222A, which has excellent saturation characteristics. This solution proved very satisfactory.

4.2 THRUST LEVEL SELECT D-to-A CONVERTER CIRCUIT

The original circuit uses resistive dividers connected between ground and a 6.2V zener diode. The disadvantages of this circuit are considerable loading of the flip-flops (about 4 mA worst case) causing unreliable operation of the turn on steering capacitor networks, and the fact that the isolating diodes (CR 11, CR 16, CR 17, CR 18 in A12) are directly in series with the low-voltage output, causing considerable temperature variation in the thrust reference level.

The Mk II circuit (Fig. 5) alleviates both of these problems with no overall increase in complexity. The heaviest load on any transistor is about 335 μA and the temperature stability of the output is fairly good, especially at the 20 μlb level. Data are shown in Table IX. Basically the circuit is a programmed current source. Three of the four resistors are grounded by the flip-flop collectors and thus subtract current from the summing point. The state of the flip-flops determine which resistor does not conduct and therefore controls the output current and voltage.

TABLE IX

OUTPUT VOLTAGE vs TEMPERATURE FOR D-to-A CONVERTER

	MK II			MK III With 4 Comp. Diodes			MK III With 5 Comp. Diodes		
STEP	-20°C	+25°C	+80°C	-20°C	+25°C	+80°C	-20°C	+25°C	+80°C
1	.389	.377	.352	.304	.313	.318	.322	.329	.331
2	.645	.637	.614	.614	.628	.637	.651	.659	.663
3	.888	.885	.865	.906	.923	.933	.961	.969	.971
4	1.16	1.16	1.15	1.22	1.25	1.26	1.30	1.31	1.31

Another D-to-A converter circuit (Fig. 6) was developed in an attempt to achieve better temperature stability. This was done, but at the price of more components and higher worst case collector loading (about 0.73 mA) in the flip-flops. This circuit, referred to here as Mk III, does not sum currents but merely gates different resistors into the current source emitter. The saturation voltages of the flip-flop transistors have no effect, therefore, and temperature stability is very good. This is the circuit configuration which was finally chosen.

4.3 OVERLOAD AND CONVERTER DRIVE CIRCUIT

A new high voltage overload circuit was breadboarded which senses I^+ and I^- by monitoring the voltages across resistors placed in series with the existing 1K resistors used to provide beam current information. As might be expected, the large transients and stray capacitances present in the HV rectifier circuits combine to produce very dirty waveforms across these new resistors. The relatively high impedance of the sensing circuits used, however, permits easy filtering of the signal, and accurate monitoring of the actual load current is achieved. The + and - 12V supplies are used as voltage references. This allows a very repeatable overload trip level. The signals from the overload sensors trigger a one-shot which turns the HV converter off for a fixed period, nominally 7 msec. If the overload condition is still present at the end of that time, the HV converter comes on for a time determined by the severity of the overload. In the case of a complete short (or a typical arc), the "on" time is determined by the time constant of the sensing circuits' noise filter. The "on" time in this case is something like 200 or 300 μsec.

Testing of the overload circuit was initially plagued by a tendency of the HV converter to enter a high-frequency mode. In some cases it would

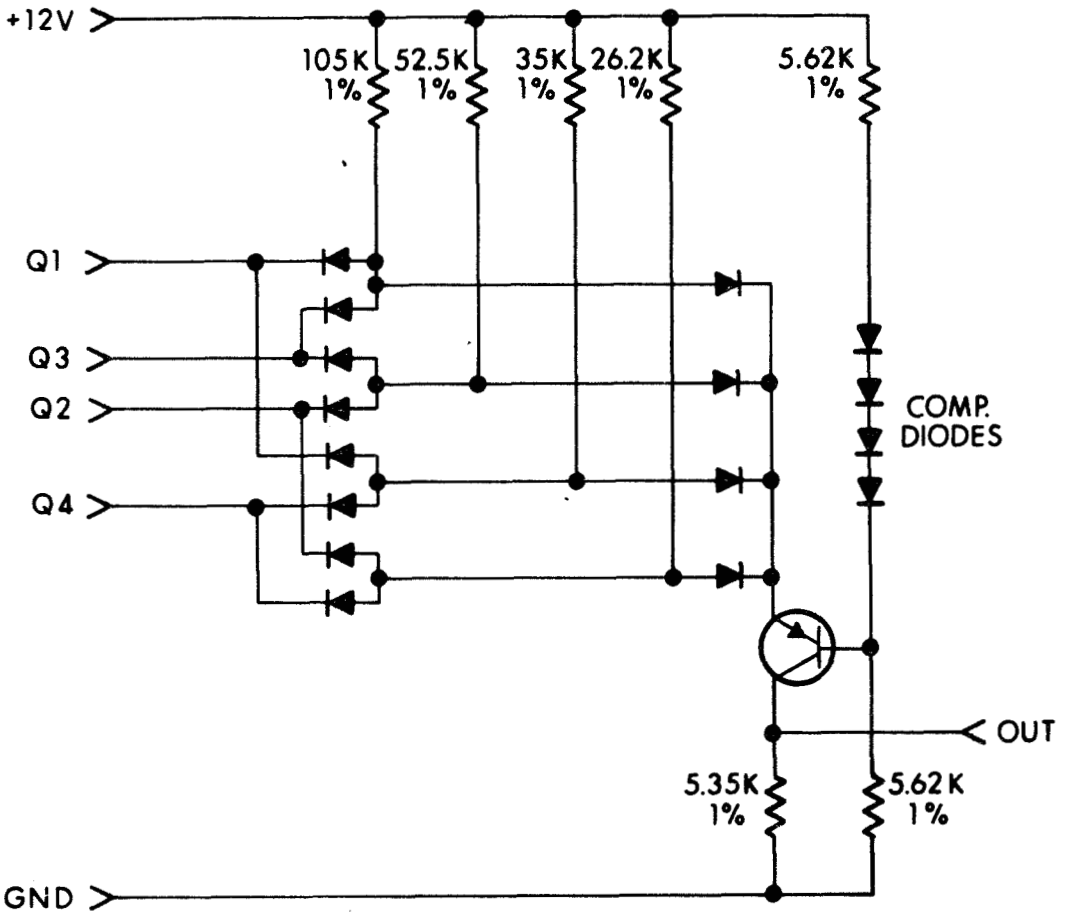

Figure 6. Digital-To-Analog Converter Circuit

maintain this mode, drawing heavy current from the supply, until the supply was turned off. This was due to the fact that the HV output is too low in this mode to provide enough current for the overload circuit to sense.

At first, this mode was associated with the turn-off method (transistors shunting the base drive to the converter transistors) and alternate methods such as electronically disconnecting the 910 ohm "starting" resistor were tried. The high-frequency mode problem persisted, however, and it became obvious that the turn-off method was not at fault.

In the normal mode, all base drive must pass through the 910 ohm "starting" resistor. The high-frequency mode, however, is sometimes maintained when this resistor is disconnected. Drive current to each base must therefore be supplied by the opposite base or by components connected to it. However, disconnecting the 0.01 μF capacitors that normally shunt the bases did not stop the high-frequency mode. The main source of base drive in this mode, therefore, appears to be stored charge possibly coupled with the effects of base-to-collector capacitance.

Several methods were tried to alleviate the problem. The most promising was to slow down reversal of base drive current by connecting 100 μH inductors in series with existing 68.1 ohm resistors. This effectively eliminated the high-frequency mode. However, since it delayed the turn-off of each converter transistor as well as the turn-on, the converter transformer was driven further into its saturation region each half-cycle, and switching losses increased to an intolerable extent.

This was avoided by the addition of diodes, as shown in Fig. 7. With the diodes connected, the turn-on of each converter transistor is delayed by the inductor, but the turn-off is very fast. Switching losses are improved even over the original configuration (by more than one watt on the breadboard) and the high-frequency mode is prevented.

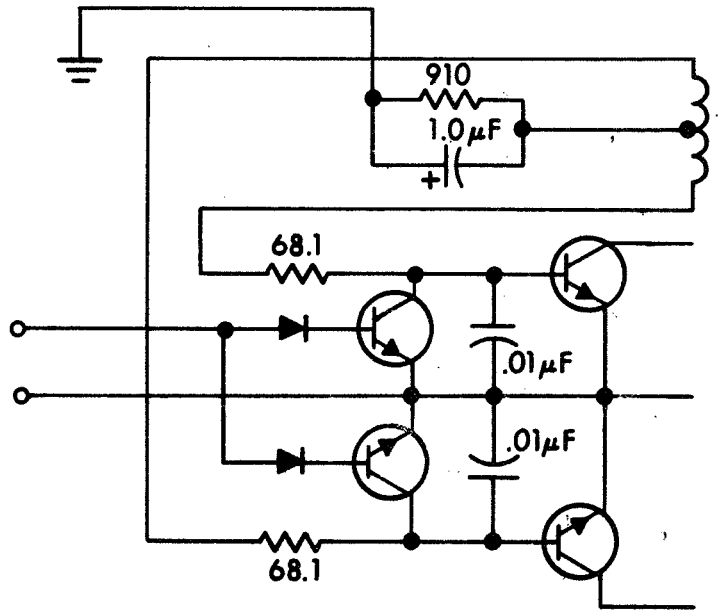

a. Original

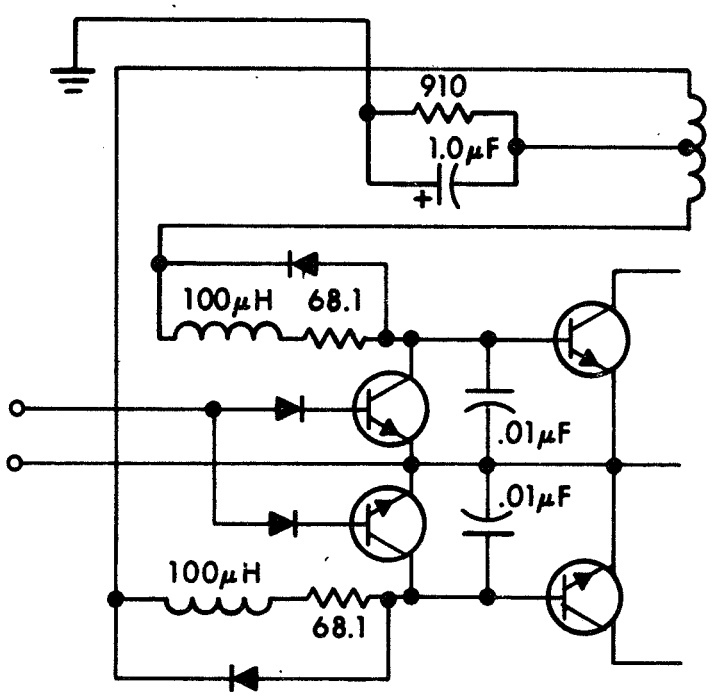

b. Modified

Figure 7. Overload and Converter Drive Circuit

4.4 CONSTRUCTION AND TESTING OF BREADBOARDED MODULES

In order to facilitate temperature measurements and to ensure compatibility with the CLPC, it was decided to build plug-in breadboards with size and layout similar to the final encapsulated modules. Testing the flip-flops in the A12 module was considered to be an adequate substitute for testing the deflection counters in the A6 and A7 modules. Therefore, breadboards of only the new A12 and A13 modules were constructed. As far as possible components identical in type to those in the original modules were specified. Some components of the proper types were already available from ATS prototype stores and these were used where possible.

In addition to these flight-type (but unscreened) components for the welded modules, some components of different types were used in the construction of the plug-in breadboards of the A12 and A13 modules. These consisted mainly of carbon composition resistors and RN60-type metal film resistors. The carbon resistors were used where circuit performance did not depend on a precise value. The RN60 types, which have a tolerance and temperature coefficient essentially the same as the Angstrohm flight resistors, were used in critical points in the circuits such as the thrust level reference d-to-a converter.

The construction of the plug-in breadboards of A12X and A13X was completed and testing was begun using CLPC S/N 04. (The X designation is used to distinguish between original and modified module designs.) Several problems remained to be overcome before meaningful environmental tests could be run. The overload one-shot circuit in A13X displayed a recovery time of about 2.2 msec. This was not acceptable since it represents the "on" time of the high voltage converter during heavy overloads. The excessive time was largely due to a 10K resistor connected between C16 and CR18 to eliminate triggering of the one-shot due to transients

from the -24V supply. Several alternate methods were tried to eliminate the transient problem, including an emitter follower from R9, but the best solution appeared to be to apply a filtering network directly to the source of the problem, as shown in Fig. 8.

During testing of the A13X overload circuit, it was discovered that R11, the 50K resistor in the V^+ supply lead had failed. When V^+ was shorted to ground, the 3 kV charge on the capacitors in the voltage doubler was applied directly to the I^+ sensing resistor.

In the old current sensing system, the 10 μF filter capacitor across this resistor would probably absorb the charge without damaging anything. The new system, however, has no corresponding capacitor and the 3 kV appeared across the sensing resistor and arced to an adjacent pin which happened to be A14-19. As a result, the vaporizer control circuitry in the module failed.

When the cause of the problem was discovered to be the 50K resistor, it was removed and replaced with two 1/2 watt carbon 24K resistors. After this, when the V^+ supply was subjected to a complete short-to-ground, the converter would enter a high-current mode, drawing about 2 A, and would not cycle. It would cycle normally, however, if the overload was a resistor of about 100k or greater.

After considerable investigation, it was concluded that there existed a range of values of resistance which, when connected as an overload, were low enough to reduce the loop gain of the converter to near unity at a low level of oscillation and high enough to limit current from this feeble oscillation to a value below the overload trip point. This range apparently included 50K. The converter transistors, in the meantime, were turned on very hard by the dc in the 910Ω bias/starting resistor.

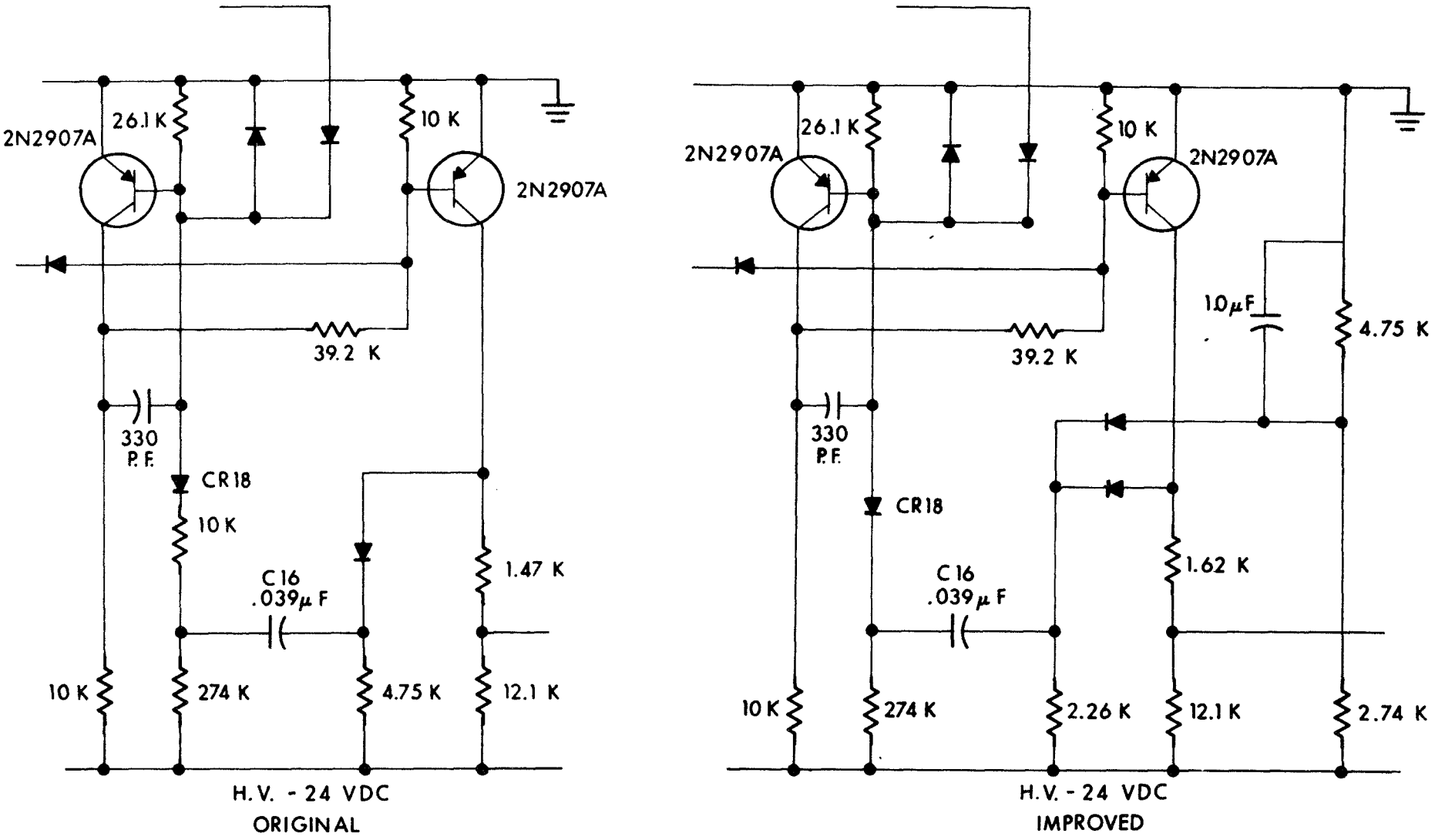

Figure 8. Breadboard A-13

The same circuit had not produced the same phenomenon with the transformer on the old system breadboard. Apparently, the poor distributed capacitance characteristic of the HV converter transformer in CLPC S/N 04 was the cause.

With this conclusion, it was decided not to spend further time trying to compensate for problems specific to a particular unit, but to press on toward a general solution. Since many if not most of the problems with the HV converter are due to its self-excited mode of operation, it is generally agreed that future units will employ a driven converter to allow more control over its operation.

It was possible to change the HV converter from the self-excited to the driven mode because its normal frequency is about 9 kHz and that of the ionizer converter is about 13 kHz. Therefore, if the HV converter were driven with energy from the ionizer converter there would be no danger of core saturation. A small transformer was designed and wound, and its primary was connected between the collectors of the ionizer converter.

This configuration operated as expected, eliminating all instability problems in the HV converter and overload circuit. It was decided to retain this circuit for remaining tests and for use with the final encapsulated modules, the only difference being that the drive transformer would be mounted under the module mother board in the final system rather than being inside the module. The only drawback to this circuit was its higher current drain. Networks previously used in the base circuits to reduce collector current overlap had no appreciable effect. Similar driven converters have been built before and operated with good efficiency, so the problem here is suspected, again, to be due to this particular converter transformer.

The A12X breadboard operated as expected except that the thrust reference level could not be made high enough to obtain a realistic 20 μlb beam current. Even when R30, which shunts the reference voltage output, was removed entirely the thrust reference level was not high enough. This yielded about 860 μA maximum beam current instead of the desired 970 μA. Since the circuit could be modified to provide this much additional current with no problems, it was decided to proceed with testing using the 860 μA level. (After the tests, it was discovered that a 10K resistor, previously connected to reduce the thrust from 20 μlb to 16 μlb, was still connected on the mother board.)

A functional test of the A12X and A13X breadboard modules was run using CLPC S/N 04 and the prototype ion engine simulator. The unit was tested on the bench and allowed to run for about five hours. All CLPC functions were exercised and worked well. Considerable sparking, in all modes, produced no change in thrust level. Transients on the TM lines due to converter switching were measured at the CLPC end of the TM cable, with full X and Y deflection and full thrust, and the highest levels found were +2.0, -2.2V on channel 14 (without external filtering).

The same system was subjected to a complete temperature test, with the ambient held at about 25°C, 70°C and 0°C. Each temperature was allowed to stabilize for about one hour, and the system was run at each temperature for about 45 minutes. No problems were encountered; the breadboards operated as expected. The beam current regulation was quite acceptable, varying from 3.20V (TM) at 0°C ambient to 3.24V at 70°C ambient. The thrust level select circuit came on at 5 μlb every time and was exercised frequently.

On the basis of these tests, the schematics for the modules were finalized.

4.5 WELDED MODULE FABRICATION AND FINAL TESTING

While complete electrical and thermal screening of components was not considered appropriate for fabrication of these nonflight modules, it was agreed that each component would be given a simple electrical test. All resistors and capacitors were therefore measured on an impedance bridge and the few whose values appeared marginal were replaced. The transistors were similarly tested on a curve tracer.

The modules (A6X, A7X, A12X, A13X) were fabricated by WEMS, Inc. using the procedures employed during the fabrication of ATS flight hardware. Appropriate modifications were made to the test fixtures and testing was conducted using similarly modified procedures.

After most of the ionizer contamination investigations had been completed, the modifications to CLPC S/N 04 were removed and the driver transformer for the high voltage converter was installed. Rather than attempting to remove the I^+ and I^- current transformers, which are not needed with the new overload sensing circuit, their secondaries were shorted at A13. All other changes necessary to make the CLPC compatible with the new modules had been accomplished earlier in order to test the breadboard modules.

All four new modules were installed in CLPC S/N 04 with the prototype air/vac simulator again used as a load. The system operated as expected with three exceptions:

a. V^+ to ground arcs caused changes in thrust level status.

b. The "off" duty cycle during V^+ or V^- overload is about 80 to 85% instead of the nominal 90%.

c. During normal nonoverload operation, with or without thrust, the overload circuit triggers in an erratic manner with no apparent cause.

Of these problems, the third was considered the most serious, and considerable effort went into seeking its solution. The -24V and ±12V lines into the module were bypassed with additional capacitors. The input and output signal leads were similarly bypassed. The module was heated and cooled over a large temperature range, and then shielded completely in copper foil connected to local ground. These and other measures had no effect on the erratic triggering. Substituting the breadboard A13X eliminated the triggering.

Finally, the encapsulated A13X module was removed from the CLPC and connected by itself to the required voltages; its output was monitored with an oscilloscope. The erratic triggering was still present. Large changes in supply voltage had no effect and the module did not respond to thumping or rapping. The problem is concluded to be due to a faulty component.

Analysis of the circuit configuration and of the test results suggests that the most likely culprit is C17, the 1 μF tantalum capacitor used as a filter in the one-shot circuit. If this capacitor were leaky as well as erratic, it would also cause the low duty cycle problem. Comparison of the "on" and "off" times produced by the breadboard module and by the encapsulated module show that the decrease in duty cycle is due to a reduction in "off" time, with the "on" time remaining fairly constant. This is precisely the effect that would be produced by leakage in C17.

Investigation of the thrust level status changes showed that transients from the V^+ to ground arc were causing the command interface circuit to produce command-like signals. The fault was not in the new A12X module. As stated at the beginning of Section 4, the poor transient immunity of the command interface circuits has been recognized for some time; but it was deliberately excluded from the scope of this investigation. Since the problem can be cured in straightforward fashion in future systems, no further attention was given to it.

None of these problems was serious enough to prevent complete temperature tests and these were run without further trouble. Due to the desire to use CLPC S/N 04 in the remaining ionizer contamination tests, and to the very limited time remaining in the program, no attempt was made to cure the A13X problem. For the ionizer tests, the breadboard module was substituted for the erratic encapsulated module, and the CLPC operated well with an actual ion engine instead of the simulator.

SECTION 5

BEAM CONTROL LOOP TRANSIENT RESPONSE

5.1 INTRODUCTION

On several occasions, particularly during the first part of a microthruster system test, the response of the beam control feedback loop has been lightly damped or oscillatory (undamped). The portion of the program reported here was concerned with an investigation of transient response prompted by the occasional periods of instability just mentioned. The approach taken was to determine gain and phase versus frequency characteristics separately for the thruster subsystem and the power conditioning and control circuitry. With this information, an evaluation of the stability of closed loop operation can be made.

5.2 CONTROL CIRCUITRY RESPONSE

The analysis of the vaporizer control loop involves the gain-phase-frequency characteristics of the circuitry which measures the beam current and adjusts the vaporizer heater current. The dynamic gain of the control circuitry can be expressed as $\Delta I_{VAP}/\Delta I_B$.

A cursory examination of the control circuit resulted in the assumption that the only significant time constant was that produced by R2 in A14 and by C13 and R37 which are mounted on the CLPC chassis. This network produced a high-frequency roll off characteristic which extended indefinitely, allowing the phase shift to approach 90°.

A more thorough analysis, however, revealed that the noninverting type of integrating circuit, which is used here, attenuates high frequencies

only down to unity gain. Higher frequencies are not attenuated further and, as a consequence, the phase shift reaches a peak and then decreases again, approaching zero at very high frequencies. The calculated gain and phase shift are shown in Fig. 9.

To simplify the measurements, the transfer characteristic of the vaporizer saturable reactor (magamp) was treated separately. The amplifier circuitry in A14 (Q1, AR1, AR2, AR3) was then breadboarded so that the measurements would not depend on the availability of a complete CLPC, and also so that all points in the circuit would be accessible.

The magamp characteristics were measured using the complete CLPC, so that the drive power (from the high voltage converter) would be realistic. A 3.10 ohm resistive load was used with a true-rms meter monitoring the output current. The bias voltage was then varied to provide data on the magamp transfer characteristic. These data are plotted on Fig. 10. The slope of this curve at 900 mA yields a dynamic transfer impedance of 3.125Ω, which is taken as typical of real operating conditions.

Since the magamp operates at a frequency of about 10 kHz, its phase shift at the frequencies of concern here (1 Hz maximum) is insignificant. The phase shift measurements were therefore confined to the amplifier circuitry, and the output measurements were made at the point which normally drives the magamp. This output point and the input signal were both connected to a variable-speed chart recorder. The input signal was provided by a Hewlett-Packard model 202A low-frequency function generator, which allowed measurements at frequencies as low as 0.006 Hz.

A second set of gain data was provided by monitoring the input and output with an oscilloscope (and with a digital voltmeter at the lower frequencies). These data matched the chart recorder data very closely. The gain and phase shift data from the chart recorder are shown in Fig. 9.

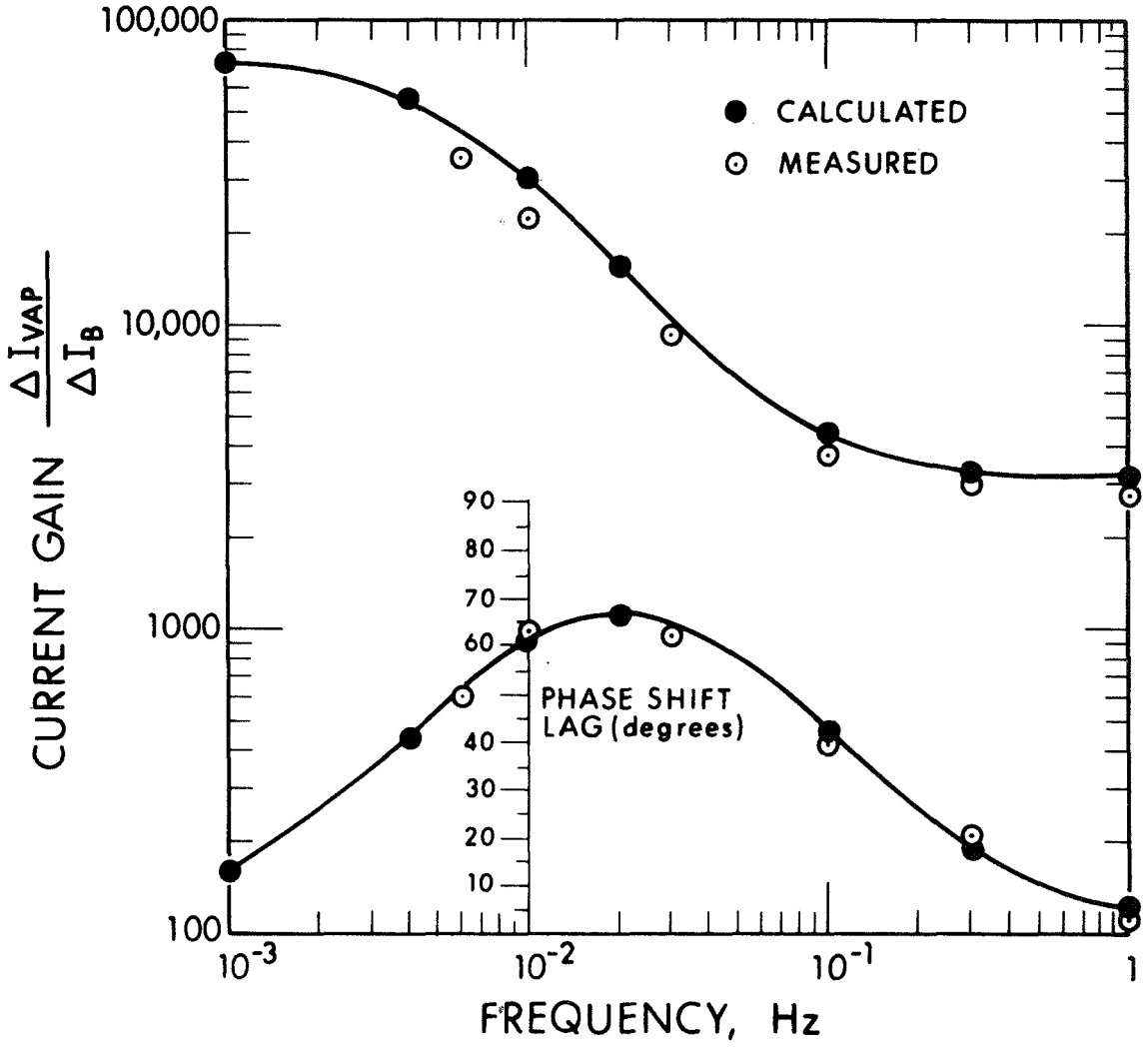

Figure 9. Vaporizer Control Circuit Gain and Phase versus Frequency

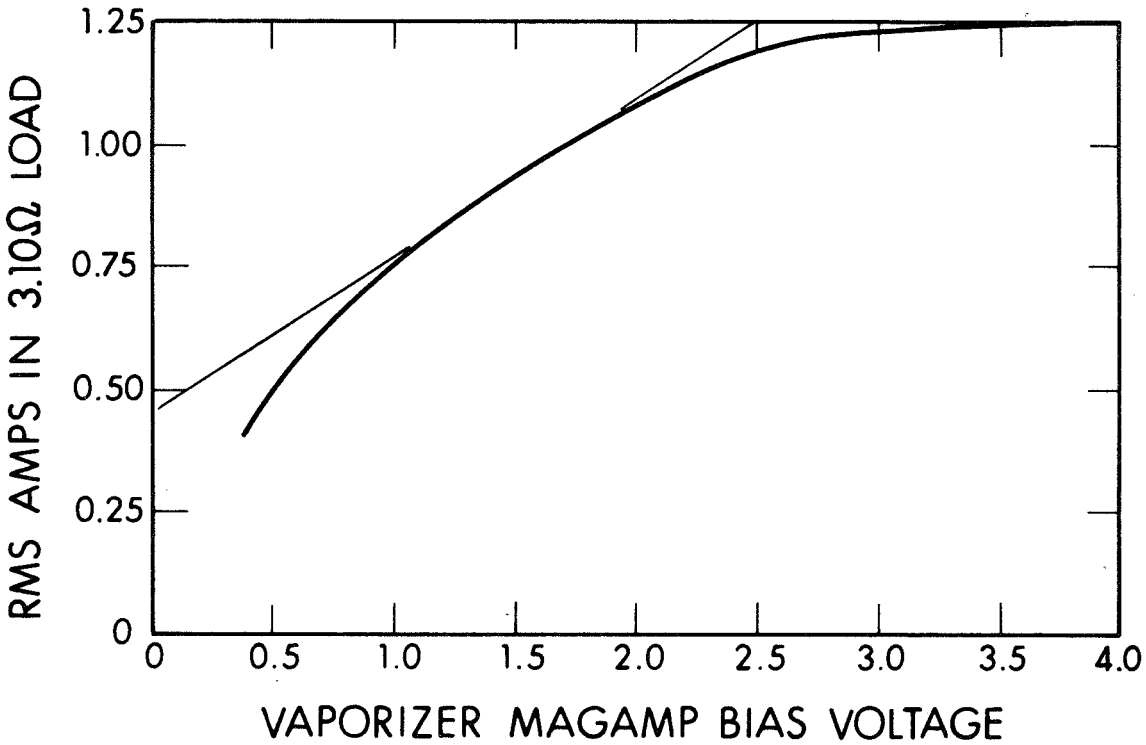

Figure 10. Vaporizer Magamp Transfer Characteristic

5.3 FEED SYSTEM RESPONSE

The response of the microthruster feed system was similarly determined to provide data for control loop analysis. To be consistent with the control circuitry measurements, the transfer function was taken to be the ratio of beam current change to vaporizer current change, or $\Delta I_B/\Delta I_{vap}$.

To acquire the data, the vaporizer heater current was modulated between approximately 0.75A and 1.25A. The frequency of modulation was varied between 0.4 Hz and 0.005 Hz. The modulation produced peak-to-peak ion beam current variations between 200 μA and 4 μA. The relatively large change in vaporizer current, ΔI_{vap}, was necessary to allow accuracy at the higher frequencies measured. Some data were taken at ΔI_{vap} = 0.2A and 0.01A, but resulting changes in ion beam current ΔI_B were too small to be measured accurately. Mean ion beam current was maintained below 800 μA to avoid thruster performance problems such as "roll-over" during measurements.

Two different thrusters were tested, providing information on the variation from unit to unit. Approximate upper and lower bounds for phase shift and gain as a function of frequency are plotted in Fig. 11. The gain falls off very rapidly above 0.2 Hz; below 0.01 Hz it is approaching the steady state value of approximately 1000 μA ion beam per ampere of vaporizer heater current. The difference between the upper and lower phase shift curves is approximately 45°; the corresponding difference in gain is 150×10^{-6} at 0.01 Hz.

The feed system response data were collected in the following manner. A thruster was assembled with a new feed system. After wick wetting, the thruster was operated for approximately 100 hours during critical temperature measurements for the ionizer contamination portion of the

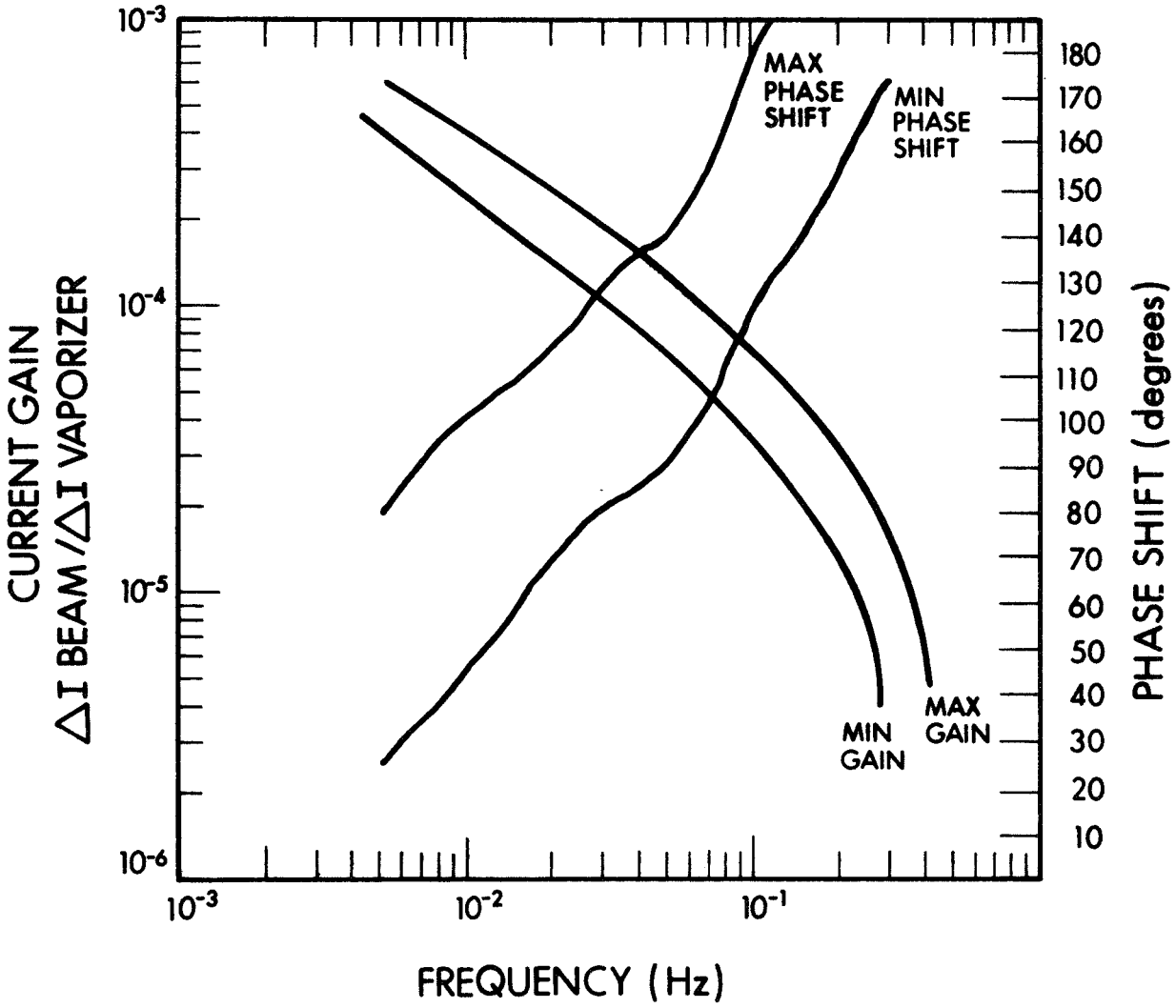

Figure 11. Vaporizer Gain and Phase versus Frequency

program. At the time feed system data were collected. The thruster was operated another 50 hours, and data were again taken. The thruster was turned off for 25 hours but remained under vacuum. The thruster was started and operated for 25 hours and data were again taken. These data are shown in Figs. 12 and 13.

The second set of data was collected with another thruster. Measurements were made immediately after wick wetting, and again after 50 hours of operation for ionizer studies. Results are shown in Figs. 14 and 15.

The data indicate a reduction in phase shift with time, and also a reduction in gain with time. The latter effect is less clear however. Both trends were toward more stable operation which is consistent with observed behavior.

The feed system response data had the following two unexpected features: (a) a large variation between sets of data, and (b) large phase shifts were observed. Earlier work suggested that the feed system response might be that corresponding to a single integrating time constant in which the thermal mass of the valve-reservoir assembly corresponded to the capacity of an RC network while the conductive losses to the reservoir corresponded to the resistance. Under these circumstances, the maximum phase shift observed would be 90 degrees. Since phase shifts exceeding 200 degrees were observed, a more complex model was clearly required.

First, an attempt was made to fit typical data empirically. The transient response of the system and the linear phase shift characteristic over a wide frequency range suggested that the response be represented by an integrating time constant plus a delay. The delay contributes a phase shift linear with frequency but contributes nothing to the amplitude response. The integrating time constant contributes a phase shift which approaches 90 degrees asymptotically and the familiar 6 db per

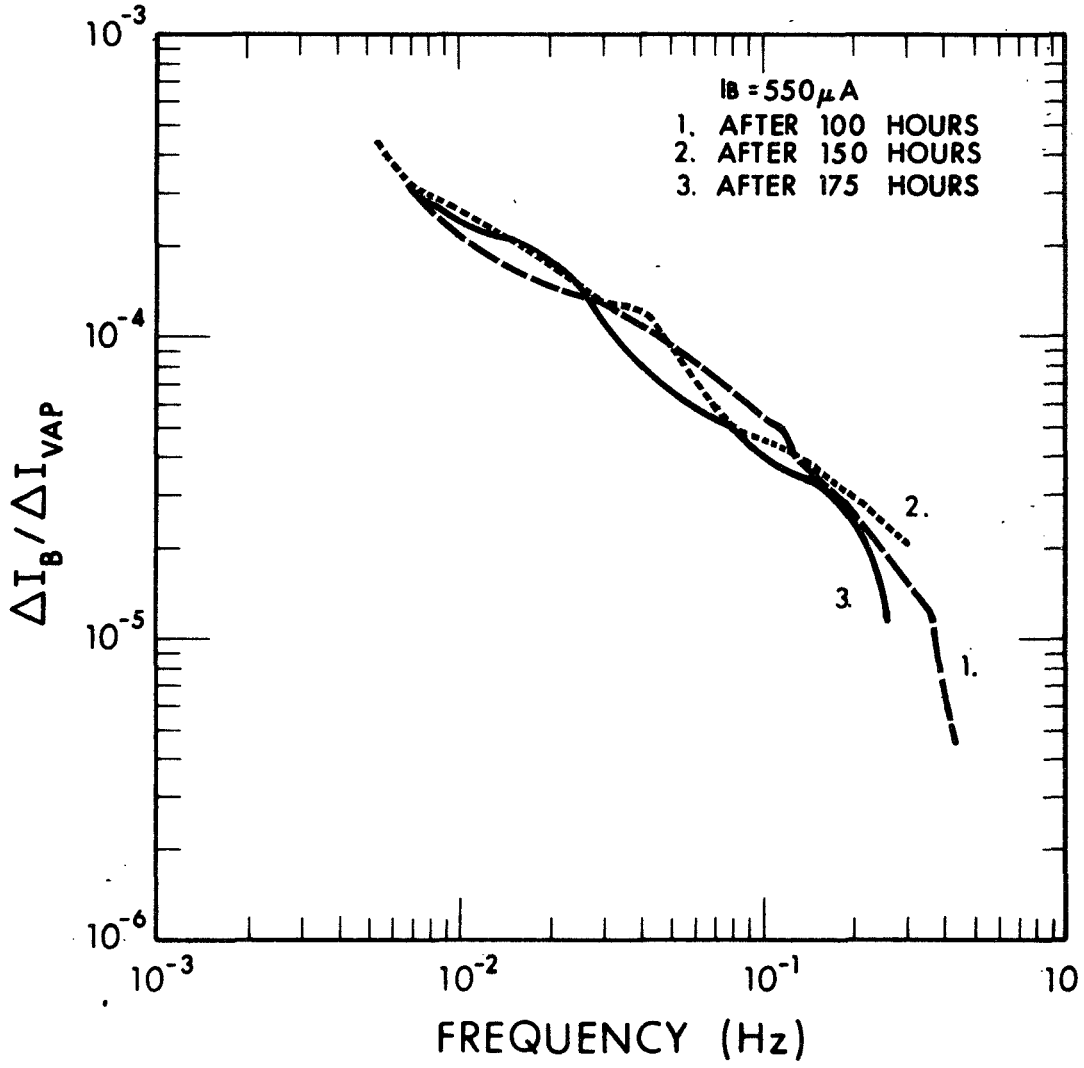

Figure 12. Vaporizer Phase Response

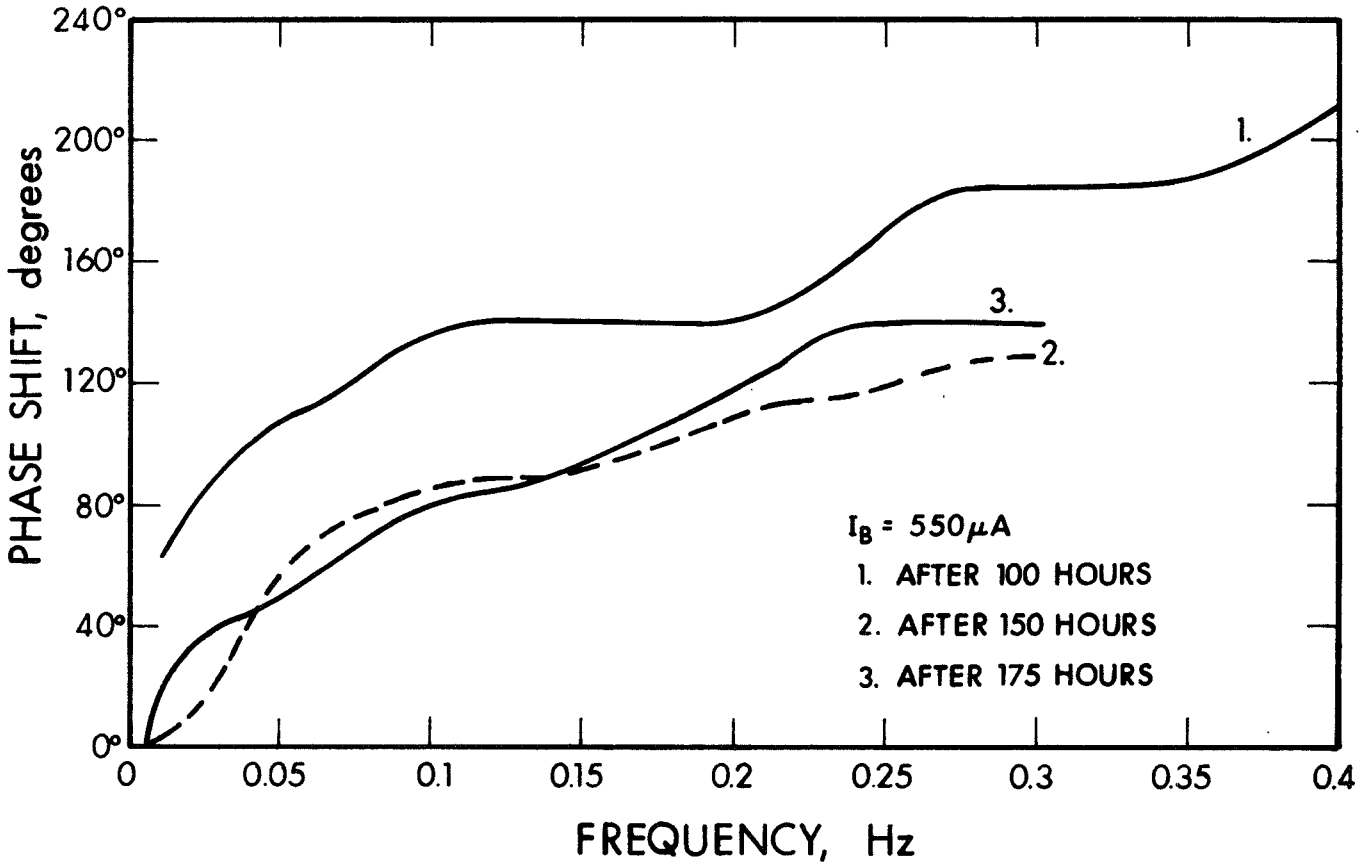

Figure 13. Vaporizer Amplitude Response

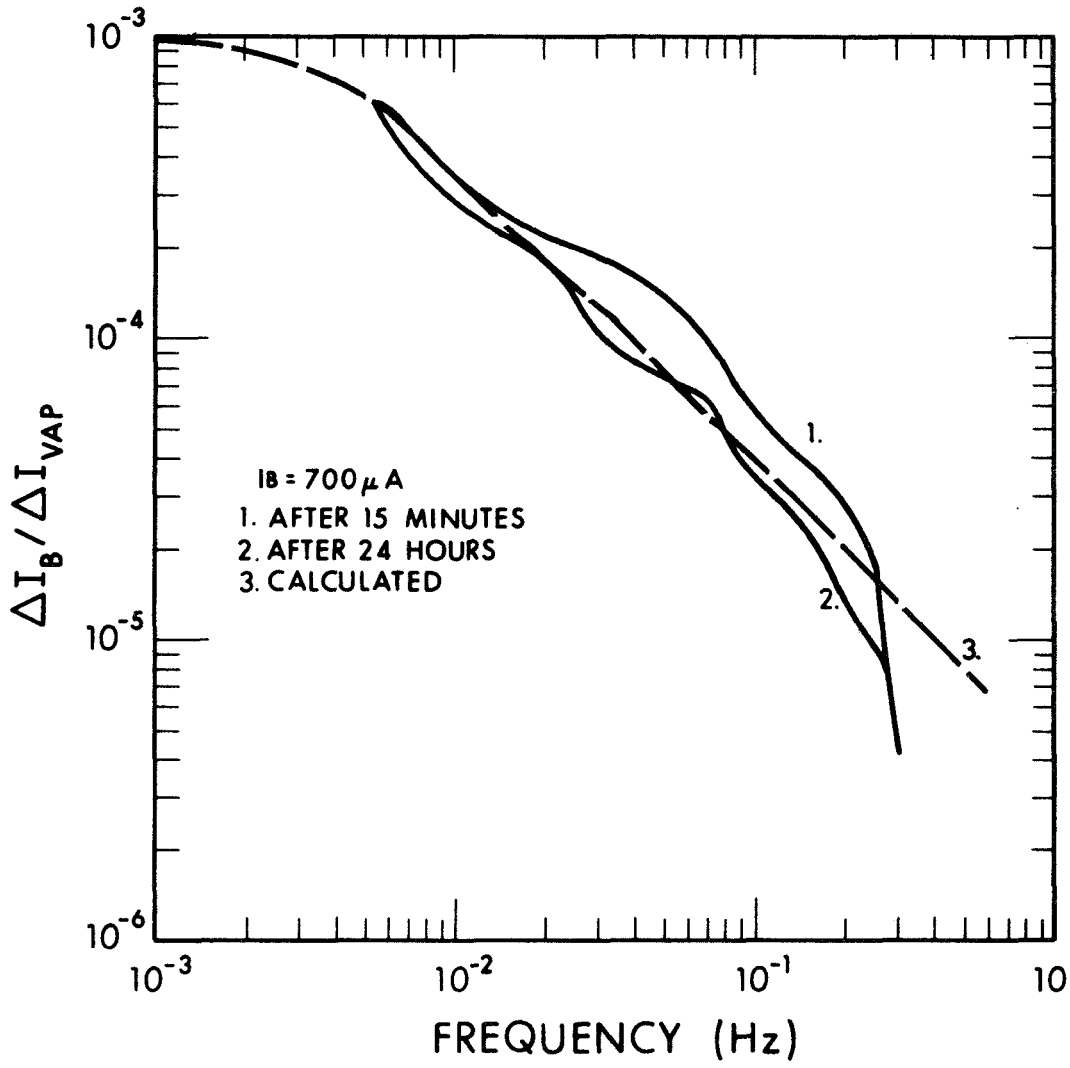

Figure 14. Vaporizer Phase Response

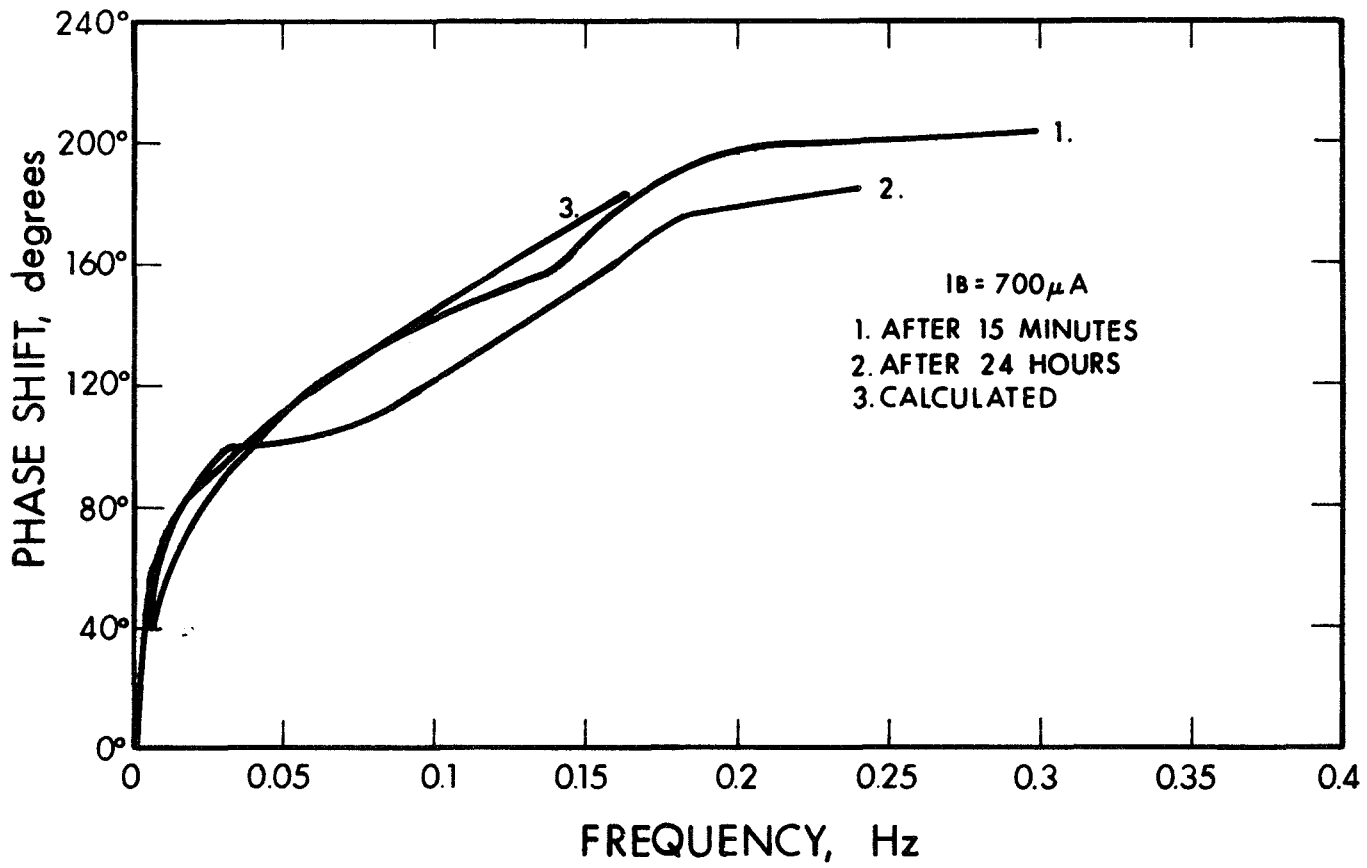

Figure 15. Vaporizer Amplitude Response

octave roll off above the characteristic frequency. Response curves based on a 40-second time constant and a 1.6-second delay are shown in Figs. 14 and 15. While not exact, the representation is reasonably good. Although useful in terms of data analysis, this interpretation lacks a physical basis because there is no obvious way to realize a pure delay in a system of this type.

In an attempt to provide a better physical representation, it was decided to investigate the response of a distributed system by solving the partial differential equation for heat conduction in one dimension. The basic equation is the familiar diffusion equation:

$$A^2 \nabla^2 U - \frac{\partial U}{\partial t} = 0$$

By separating variables and choosing a solution period in time, a one dimensional solution of the following form may be found:

$$U = U_o \exp\left[-\sqrt{\frac{\omega}{2a^2}}\, x\right] \exp\left[i\left(\sqrt{\frac{\omega}{2a^2}}\, x - \omega t\right)\right]$$

By applying the boundary condition that sinusoidally varying, constant amplitude power is applied at x = 0, the amplitude and phase responses may be expressed as

$$\text{Amplitude} \sim \frac{\text{const.}}{\sqrt{f}} \exp\left[-\sqrt{\frac{\omega}{2a^2}}\, x\right]$$

$$\text{Phase (rad.)} = \sqrt{\frac{\omega}{2a^2}}\, x$$

This model is less successful in fitting the experimental data. It does not account for the large phase shift at frequencies below 0.05 Hz or the more or less linear phase shift above 0.05 Hz. The amplitude response has the proper qualitative behavior, but it does not fit the data as well as the single time constant calculation.

The measured gain and phase shift characteristics of the control electronics were combined with the corresponding characteristics of the thruster; the result is shown in Fig. 16. The thruster data were in the form of boundaries, so the combined data also represents minima and maxima rather than specific examples.

These curves represent the open-loop characteristics of the complete control loop. They indicate that, in most cases, the loop is stable and will not oscillate; but it will exhibit ringing when excited by a transient or a command to a new thrust level. This ringing will have a period between roughly 20 sec and 100 sec. The curves also indicate, however, that worst-case systems will oscillate with a period somewhere in the same range. These conclusions are in agreement with experimental system test results. In these results it has been observed that on isolated occasions the feed control loop is unstable and oscillates for a period of hours before becoming stable.

This marginal stability is apparently due to the very large phase shifts associated with the thruster vaporizer response. Three approaches might be investigated in producing a more nearly ideal control loop:

a. Gain reduction - Zero frequency loop gain is approximately 100. This is probably higher than necessary to provide stabilization against fluctuations in vaporizer characteristics. While a gain of 30 to 50 would probably be adequate, the gain would have to be lowered to approximately 20 to provide stability in the worst case.

b. Loop compensation - Only the simplest (lag network) has been tried. More sophisticated forms of compensation would give improved results.

c. Vaporizer redesign - Occasional instability could be avoided by reduction of the large vaporizer phase shifts; this appears to be an attractive possibility, but it could not be investigated during this program. It has been suggested that the large phase shifts may be associated with condensation and reevaporation of cesium from internal surfaces of the feed line valve.

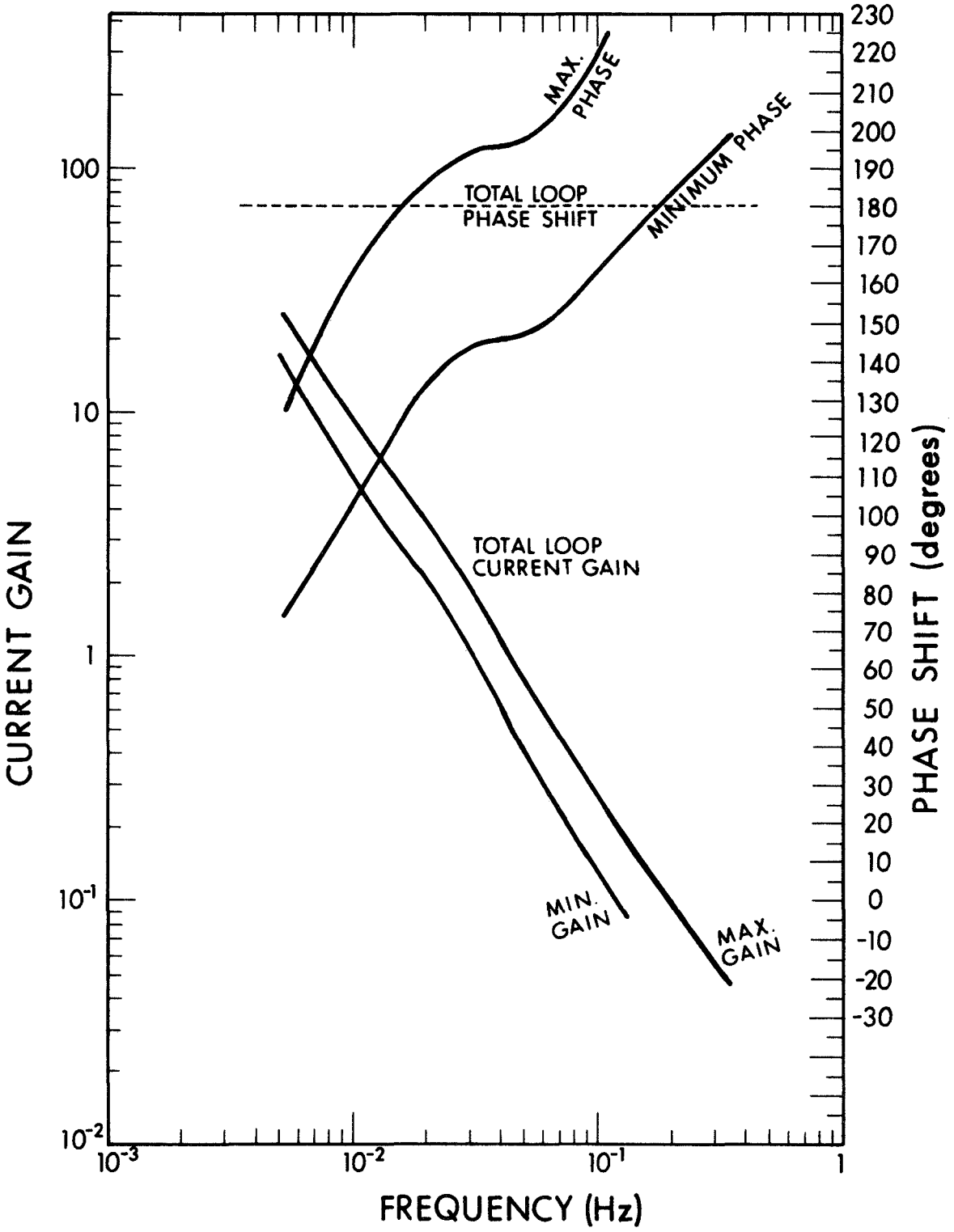

Figure 16. Vaporizer Control Loop Gain and Phase Shift Limits

SECTION 6

NEW TECHNOLOGY

In the process of evaluating candidate materials for porous tungsten ionizer protective coatings, it was found that Styron 666U (polystyrene manufactured by Dow Chemical Corporation) possessed the following characteristics which make it useful as a protective coating material:

a. Can be applied by dissolving in solvent methyl ethyl ketone and applying with brush

b. Reduces gas flow permeability of ionizer to less than 1% of original value

c. Is stable for long periods in laboratory environment

d. As the ionizer is heated to operating temperature (1150°C), the coating decomposes and evaporates, leaving the ionizer with original vapor flow permeability and with surface properties appropriate for surface ionization of cesium.

REFERENCES

1. H. Shelton, "Experiments on Atom and Ion Emission from Porous Tungsten," ARS Electric Propulsion Conference, Berkeley, California, No. 2360-62, 11 p. (March 14-16, 1962).

2. O. K. Husmann, "Experimental Evaluation of Porous Materials for Surface Ionization of Cesium and Potassium," Electric Propulsion Development, Progress in Astronautics and Aeronautics, Vol. 9, New York, Academic Press, 1963, p. 195.

3. O. K. Husmann, "A Comparison of the Contact Ionization of Cesium on Tungsten with that of Molybdenum, Tantalum and Rhenium Surfaces," AIAA Electric Propulsion Conference, Colorado Springs, Colorado (March 11-13, 1963).

4. H. Shelton, "Research and Development of Porous Tungsten for Use in Electrostatic Propulsion," NASA Contract No. NAS 8-41, 8942-6025-Ru-000 (March 20, 1963).